Ecologically distinct myodocope ostracod faunas from a single horizon in the late Silurian of Spain

Vincent Perrier, Gwendal Perrichon, Félix Nesme, Helga Groos-Uffenorde, Saturnino Lorenzo, Juan Carlos Gutiérrez-Marco

Ecologically distinct myodocope ostracod faunas from a single horizon in the late Silurian of Spain

Des faunes d'ostracodes myodocopes écologiquement distinctes provenant d'un même horizon du Silurien supérieur d'Espagne

Vincent PERRIER [1*], Gwendal PERRICHON [1], Félix NESME [2], Helga GROOS-UFFENORDE [3], Saturnino LORENZO [4], Juan Carlos GUTIÉRREZ-MARCO [5]

[1] Université de Lyon, UCBL, ENSL, CNRS, UMR 5276 LGL-TPE, 69622 Villeurbanne, France; e-mails: vincent.perrier@univ-lyon1.fr, gwendal.perrichon@univ-lyon1.fr

[2] Institut des Sciences de l'Evolution, Université de Montpellier, UMR5554 CNRS, IRD, EPHE, Place Eugène Bataillon, CC65, 34095 Montpellier Cedex, France; e-mail: felix.nesme@umontpellier.fr

[3] Geowissenschaftliches Museum, GZG, Georg-August-Universität Göttingen, Goldschmidt - Str. 3, 37077 Göttingen, Germany; e-mail: hgroos@gwdg.de

[4] Dpto. Ingeniería Geológica y Minera, Escuela de Ingeniería Minera e Industrial de Almadén-IGeA (UCLM), Plaza Manuel Meca 1, 13400 Almadén, Ciudad Real, Spain; e-mail: saturnino.Lorenzo@uclm.es

[5] Instituto de Geociencias (CSIC-UCM) and Área de Paleontología GEODESPAL, Facultad de Ciencias Geológicas UCM, José Antonio Novais 12, 28040 Madrid, Spain; e-mail: jcgrapto@ucm.es

*Corresponding author

Abstract: Silurian myodocopes have been demonstrated to be the pioneer pelagic ostracods. Their ecological shift into the water column, during the middle Silurian (Wenlock-Ludlow), is now well documented from sites around the world, but the evolution of this fauna during the late Silurian (Pridoli) remains little studied. We recognise, for the first time, two ecologically distinct myodocope ostracod faunas from the same late Pridoli horizon (possibly ?*Wolynograptus bouceki* - *Skalograptus transgrediens* Biozones) of southern Spain (Alcaracejos, province of Córdoba). One fauna, associated with black shales, comprises five species belonging to three myodocope families (bolbozoids, entomozoids and cypridinids). The other fauna, recovered from large dark-reddish calcareous nodules and associated with the planktonic crinoid *Scyphocrinites elegans*, comprises seven myodocope species belonging to same three families and include one new species, *Calocaria callundosa* sp. nov. Although the shale and nodule faunas have two species in common, they are clearly different in terms of diversity, abundance and size of the specimens. The discrepancies between these two assemblages could either be explained by sampling or taphonomic bias, or because they represent faunas with different ecologies. In the latter hypothesis, the myodocope association in the shales could represent the "background" planktonic fauna, while the fauna in the nodules could have lived in the water column in the vicinity of the *Scyphocrinites* "floating islands", or scavenge around the dead crinoids on the sea floor. These two diverse assemblages also allow discussions on the temporal and palaeogeographical distributions of these late Silurian myodocope ostracods.

Résumé : Il est aujourd'hui communément accepté que les myodocopes du Silurien étaient les premiers ostracodes pélagiques. Si leur colonisation de la colonne d'eau, au cours du Silurien moyen (Wenlock-Ludlow), est maintenant bien documenté dans des sites du monde entier, l'évolution de cette faune à la fin du Silurien (Pridoli) reste peu étudiée. Nous

décrivons ici, pour la première fois, deux faunes d'ostracodes myodocopes écologiquement distinctes provenant du même horizon du Pridoli supérieur (possiblement dans les Biozones ?*Wolynograptus bouceki* - *Skalograptus transgrediens*) du sud de l'Espagne (Alcaracejos, province de Cordoue). L'une des faunes, associée aux schistes noirs, comprend cinq espèces appartenant à trois familles de myodocopes (bolbozoïdés, entomozoïdés et cypridinidés). L'autre faune, trouvée dans de grands nodules calcaires rouge foncé et associée au crinoïde planctonique *Scyphocrinites elegans*, comprend sept espèces de myodocopes appartenant aux trois mêmes familles et inclut une nouvelle espèce, *Calocaria callundosa* sp. nov. Bien que les faunes des schistes et des nodules présentent deux espèces en commun, elles sont clairement différentes en termes de diversité, d'abondance et de taille des spécimens. Les divergences entre ces deux assemblages pourraient s'expliquer soit par des biais d'échantillonnage ou taphonomiques, soit elles pourraient représenter des faunes aux écologies différentes. Dans cette dernière hypothèse, la faune de myodocope des schistes pourrait représenter la faune planctonique « classique », tandis que la faune des nodules aurait vécu dans la colonne d'eau à proximité des « îles flottantes » de *Scyphocrinites*, ou bien se serait nourrie de manière nécrophage de ces crinoïdes morts une fois qu'ils auraient atteint le fond de la mer. Ces deux assemblages diversifiés ont également permis de discuter les distributions temporelles et paléogéographiques de ces ostracodes myodocopes du Silurien terminal.

Key words: Ostracoda, Myodocopa, paleoecology, plankton, late Silurian, Spain

Mots clés : Ostracoda, Myodocopa, paléoécologie, plancton, Silurien supérieur, Espagne

1. Introduction

The last decades of the 20th century saw the emergence of the idea that myodocope ostracods had colonised pelagic niches during the Silurian and therefore represented the earliest known record of zooplanktonic ostracods (Siveter 1984; Siveter et al. 1987, 1991; Siveter and Vannier 1990; Vannier and Abe 1992; see also Perrier et al. 2015). More recent studies focused on their systematics, functional morphology, habitats, lifestyles, biostratigraphy and palaeobiogeography (Perrier et al. 2007, 2011, 2014a-c, 2019a-c; Perrier 2012; Perrier and Siveter 2013; Mikhailova et al. 2020; Siveter et al. 2022). These studies concentrated on the colonization event itself, focusing mainly on Wenlock and Ludlow strata from various regions worldwide (UK, France, Czech Republic, Poland, Sardinia, Australia, Central Asia, Arctic Russia). Still, little is known about the latest Silurian (Pridoli) myodocopes with only a handful records in France, Czech Republic and possibly Sardinia (Perrier et al. 2011). This paper, which concentrate on a new Pridoli myodocope bearing locality, is the first of a series exploring the Silurian myodocope faunas of the Iberian Peninsula.

Myodocope ostracods, and ostracods in general, are rare fossils in the Silurian of the Iberian Peninsula, where only few species were recorded (Robardet and Gutiérrez-Marco, 2002, p. 65). They were first identified by Delgado (1908) in the late Silurian strata of the Bussaco (Sazes Formation) and Valongo areas ('Xistos Carbonosos' Formation) of the Portuguese part of the Central Iberian Zone, where this author mentioned *Bolbozoe anomala* Barrande, '*B. bohemica*' Barrande and *Beyrichia*? sp. from several horizons of shales, sandstones and fossiliferous nodules. Outside of the Iberian Massif, '*B. bohemica*' was also cited in the late Silurian of the Spanish Pyrenees (Dalloni, 1930; Schmidt, 1931), from an area where ostracods were described and illustrated fifty years later by Dégardin and Lethiers

(1982). This study focussed on a single Pridoli locality in the central Pyrenees and recorded 11 poorly preserved ostracod species, among which two are myodocopes (*i.e*. *Entomozoe* (*Richteria*) cf. *angelini* Jones and *Entomozoe* (*R*.) sp.).

Simon (1951, p. 39) discovered a different assemblage of Silurian ostracods from a thin "orthoceratid limestone" overlying graptolite shales in the Valle syncline, north of the Seville province (Ossa-Morena Zone, SW Spain). The identified taxa include *Leperditia* sp., *Kloedenia* cf. *obscura* Ulrich & Bassler, *K. intermedia marginata* Jones & Hall and *Ctenobolbina* cf. *punctata* Ulrich. These taxa form a strange 'American assemblage' associated with diverse cephalopods, Bohemian-type bivalves, gastropods, brachiopods, crinoids and abundant Wenlock graptolites. A review of the Silurian succession from this locality couldn't identify with certainty the level of provenance of the Simon's fossils, but Robardet et al. (2000, p. 270) cited the occurrence of *Bolbozoe* sp. in the "*Scyphocrinites* limestone" (Pridoli) of the Valle syncline.

Additional records of unidentified Silurian ostracods in the Iberian Massif come from different areas of the northern part of the Central Iberian Zone, such as, the Moncorvo synclinorium in NW Portugal (Sarmiento et al. 1999, p. 760), derived from Pridoli beds correlated to the "*Scyphocrinites* limestone", or a Ludfordian black orthoceratid limestone in the Caurel-Peñalba syncline, NW Spain (Gutiérrez-Marco et al. 2001, p. 250). In the Obejo-Valsequillo Domain of the SW Iberian Massif, the first reference to these fossils are the unidentified bolbozoids occurring in a Pridoli fossiliferous olistolith redeposited in the Guadalmellato Carboniferous basin east of Adamuz (province of Córdoba: Gutiérrez-Marco et al. 2014, p. 32). Within the same domain, the recent paper of Lorenzo et al. (2020) points out the existence of two other fossil localities placed in two abandoned open-pit mines to the SW and S of Hinojosa del Duque (province of Córdoba), from where they identified and

figured the species *Bolbozoe anomala* Barrande and *Sineruga insolita* Perrier (locality Mina Luisa), and *Silurocypridina calva* Perrier, Vannier & Siveter (locality Mina Las Angosturas).

In the present paper, we report a new ostracod bearing locality in Mina Guillermín (Obejo-Valsequillo Domain of the Iberian Massif), where a new upper Silurian section provides abundant and well-preserved myodocope ostracod faunas. With ten myodocope ostracod species, this locality provides a unique window on the latest Silurian representative of the group allowing discussion about their systematics, palaeobiogeography and palaeoecology.

2. Geological Setting

The studied material comes from a small Silurian section located in the Obejo-Valsequillo Domain, a complex area regarded either as the northernmost part of the Ossa-Morena Zone or as the southernmost part of the Central Iberian Zone of the Iberian Massif (see Fig. 1 and discussion in San José et al. 2004). The Domain has been recently ascribed to the Ossa-Morena Complex (Díez-Fernández and Arenas 2015), belonging to a group of allochthonous terranes of the new Galicia-Ossa-Morena Zone exposed in the southern branch of the Variscan Orogen (Arenas et al. 2016). According to this model, the Obejo-Valsequillo Domain would represent the upper allochthonous units of a large peri-Gondwanan domain, contrasting with the Central Iberian Zone that was part of the autochthonous Gondwanan marine platform (Arenas et al. 2016; Díez Fernández et al. 2016).

Sparse and isolated Silurian exposures within the Obejo-Valsequillo domain occur in less than a dozen localities, usually highly tectonised and scarcely fossiliferous (Palacios et al. 2013; Lorenzo Álvarez 2015; Aragonés-Illanas 2015; Lorenzo et al. 2020). Silurian rocks are

also recognized as small olistoliths incorporated to a Carboniferous olistrostrome in the eastern part of the domain (Gutiérrez-Marco et al. 2014). As in the remaining Ossa-Morena Zone, the Obejo-Valsequillo Domain records the development of calcareous facies (orthoceratid and scyphocrinoid limestones) in Ludfordian and Pridoli strata, which strongly contrast with the contemporaneous but much shallower siliciclastic facies and faunas of the southern Central Iberian Zone.

The Silurian section studied here rests in tectonic contact on Ordovician sandstones and comprises approximately 50m of weathered black to reddish shales intercalated with thin sandstone layers, which are only frequent in the lower and upper parts of the succession. Towards the middle part of the sequence (i.e. 15-20m above the base of the section), thin calcareous lenses and reddish calcareous nodules become locally abundant. These very fossiliferous nodules contain articulated remains of scyphocrinoids, orthoconic nautiloids, bivalves, gastropods, phyllocarids and myodocope ostracods. These nodules are embedded in black/reddish shales containing graptolites, orthoconic nautiloids and myodocope ostracods.

From the biostratigraphic point of view, the record in the nodules of the cephalopod *Kopaninoceras fluminese* (Meneghini), and in the shales of abundant poorly preserved remains of *Skalograptus* cf. *transgrediens* (Perner), are indicative of the upper Pridoli (?*Wolynograptus bouceki* - *S. transgrediens* Biozones), a range that could be correlated to the proposed Bohemian Radotinian stage (see Manda et al. 2023). Geographically, the Mina Guillermín section studied herein is located on the eastern margin of the Cañada Real Soriana (an old track for transhumance cattle) near the Guillermín mine, 7 km northeast of Espiel and 2.13 km south-southeast of Puerto Calatraveño (km 380.5 of the National Road N-502), within the municipality of Alcaracejos (province of Córdoba). The geographical coordinates for the main bed with fossiliferous nodules is Lat. 38º14´17.9˝N, Long. 4º58´11.8˝W.

3. Material and Methods

In Mina Guillermín the myodocopes occur in two different lithologies, altered black/reddish shales and reddish calcareous nodules preserving internal and external moulds and, in some rare cases, the remnant of the carapace. Rock matrix was removed from the specimens mechanically using fine needles. Casts of external moulds of all of the ostracods recovered were made with latex rubber using the technique of Siveter (1982). Specimens and casts were coated with a thin layer of ammonium chloride and photographed using a Canon MPE 65 lens mounted with a Canon EOS 5DSR camera. Stereo-pairs were extensively used. Specimens were measured using a Zeiss Discovery V8 binocular with the Axiovision 40 4.8 2.0 software.

Silurian myodocopes typically have a presumed weakly calcified bivalved carapace with a probable ligamentous dorsal connection (Perrier 2012). The internal mould of each valve in many specimens preserves an adductor muscle scar/spot subcentrally, corresponding to the site of internal attachment of the adductor muscle. The surface of the carapace may be smooth or have a range of types of ornament, including reticulation, corrugation and punctuation. The surface of the carapace in some cases shows post-mortem diagenetic features (‘rosettes’; Siveter et al. 1987). The morphological terminology used herein follows that of Siveter et al. (1987) and Perrier (2012).

Repositories for the ostracods are: Université Claude Bernard Lyon 1, France (FSL); Université de Rennes, France; (IGR); Museo Geominero/IGME-CSIC, Madrid, Spain (MGM); Národní Museum, Prague, Czech Republic (NM); Université de Brest, France; (LPB); Oxford University Museum of Natural History (OUMNH).

198

199 **4. Systematic Palaeontology**

200

201 Class OSTRACODA Latreille, 1802

202 Subclass MYODOCOPA Sars, 1866

203 Superfamily BOLBOZOOIDEA *sensu* BOLBOZOACEA Bouček, 1936

204 Family BOLBOZOIDAE Bouček, 1936

205

206 Genus ***Bolbozoe*** Barrande, 1872

207

208 *Type species*. *Bolbozoe anomala* Barrande, 1872; subsequent designation by Bassler and
209 Kellett, 1934. Ludlow Series, Silurian, Czech Republic.

210 *Other species*. *Bolbozoe acuta* Perrier, Vannier & Siveter, 2011, *Bolbozoe beccata* Perrier,
211 Siveter, Williams & Lane, 2014c, *Bolbozoe largiglobosa* Wang & Zhang, 1983, *Bolbozoe*
212 *parvafraga* Perrier, Vannier & Siveter, 2011, *Bolbozoe psittaca* Perrier, Siveter, Williams &
213 Palmer, 2019a, *Bolbozoe rugosa* Perrier, Vannier & Siveter, 2011, *Bolbozoe* sp. nov. A of
214 Perrier et al. 2019a, *Bolbozoe* sp. nov. B of Perrier et al. 2019a and possibly *Bolbozoe jonesi*
215 Barrande, 1872.

216 *Diagnosis*. Bolbozoidae with a single, anterior sulcus. Anterodorsal bulb large, occupies
217 20–25% of valve lateral surface area, tends to fuse with rostrum. Rostrum prominent or
218 reduced. Pointed caudal process present or absent. Hinge line short, situated anterodorsally
219 above bulb. Adductor muscle scar area large, rounded or reniform, with a single or double
220 series of scars. Valves tuberculate, reticulate/corrugate or smooth (Perrier et al. 2011).

221 *Stratigraphic and geographic range*. Upper part of the Wenlock Series, Silurian, to Emsian
222 Stage, Devonian; Czech Republic (Perrier et al. 2011), France (Perrier et al. 2011), Sardinia

(Gnoli et al. 2009), China (Wang 2009), Australia (Perrier et al. 2014c), Wales and England (Perrier et al. 2019a), Poland (Perrier et al. 2019b) and Uzbekistan (Mikhailova et al. 2020).

***Bolbozoe anomala* Barrande, 1872**

Figs 2A-C, 3A-E.

2019a *Bolbozoe anomala* Barrande, 1872 - Perrier et al., pl. 3, figs 1-18 (see p. 26 for full synonymy).

2019b *Bolbozoe anomala* Barrande, 1872 - Perrier et al., fig. 2A, B.

2019c *Bolbozoe anomala* Barrande, 1872 - Perrier et al., fig. 7C.

2020 *Bolbozoe anomala* Barrande - Lorenzo et al., fig. 1T.

2020 *Bolbozoe anomala* Barrande - Mikhailova et al., fig. 2D, H, I; fig. 3C, G, K, O, S.

2021 *Bolbozoe anomala* Barrande, 1872 - Mikhailova & Siveter, fig. 11m.

Type material. Lectotype (designated Přibyl 1988, p. 119), a right valve (NM-L 23572, ex. CE1194) figured by Barrande (1872, pl. 24, figs 29, 30) and Perrier et al. (2011, pl. 1, fig. 1). Paralectotype (designated Přibyl 1988, p. 119), a left valve (NM-L 13993) figured by Barrande (1872, pl. 24, figs 27, 28) and Perrier et al. (2011, pl. 1, fig. 2).

Type locality and horizon. Lochkov suburb of Prague, Czech Republic. Požáry Formation, Pridoli Series, stratigraphical division e2 of Barrande 1872 (Kříž 1992).

Material and measurements (mm). 338 specimens from the shales (280 specimens) and nodules (58 specimens) of Mina Guillermín, Spain; Pridoli, Silurian. Size range: L=2.23/H=1.59 to L=8.24/H=5.58. Lectotype: L=8.50/H=5.95.

Diagnosis. Smooth *Bolbozoe* with sub-ovoid lateral outline and rounded posterior margin lacking a caudal process. Bulb prominent. Rostrum tiny to obsolete. Adductor muscle scar

consists of single series of inclined individual scars including about six furrows (after Perrier et al. 2011).

Description. Adult valve sub-ovoid, slightly tapering posteriorly. Anterior third of valve mostly occupied by a large hemispherical bulb forming *c*. 20–25% of valve area; bulb-centre lies just above valve mid-height and well above other surface areas of valve. Maximum valve length is just above bulb mid-height; maximum valve height is at mid-length and maximum valve width is at central part of bulb. A deep, narrow sulcus surrounds the bulb posteriorly and ventrally. An adductor muscle scar occurs at mid-length within the sulcus and consist of five-six ridges and six-seven furrows. Rostrum is small, in some cases beak-like or absent. Early ontogenetic stages are more rounded in valve outline and the bulb is relatively larger than in adults.

Occurrence. Upper Wenlock to at least the middle Pridoli series; possibly also upper Pridoli Series and Lower Devonian of Czech Republic, France, Sardinia, Poland, Wales, England, Uzbekistan and Spain. If *B. jonesi* is conspecific with *B. anomala* the species range would extend into the Devonian (see Perrier et al. 2019a, c for references).

Bolbozoe* aff. *B. rugosa Perrier, Vannier & Siveter, 2011

Fig. 3F-I

Type material of B. rugosa. Holotype: a flattened right valve (FSL 710540) figured by Perrier et al. (2011, pl. 2, figs 5, 9–10).

Type locality and horizon of B. rugosa. Les Buardières, Mayenne, France (locality 7 of Perrier et al. 2011); upper Wenlock to middle Ludlow series.

Material and measurements (mm). Five specimens from the nodules of Mina Guillermín, Spain; Pridoli, Silurian. Most complete specimen (Fig. 3F-I): L= more than 7,87/H=5,58. Holotype: L=4.32/H=3.45.

Description. Valve is sub-ovoid tapering posteriorly in lateral outline. A large hemispherical bulb occupies most of anterior third of valve, with its highest point at valve mid-height. Maximum valve height is at mid-length. A narrow sulcus surrounds the bulb; it is widest near adductorial muscle scar region. Ornament covers all valve external surface except upper part of bulb; it consists of series of relatively long, possibly concentric, in some cases bifurcated, ridges and furrows, each one about 300 µm wide.

Remarks. The type material from *B. rugosa* is from the Wenlock-Ludlow (*Colonograptus ludensis* to *Lobograptus scanicus* Biozones; Perrier et al. 2011). The main difference between the type material and the Spanish specimens is the ornament organization: on the French material, ridges and furrows are oriented obliquely from anterodorsal to posteroventral on the whole valve surface; on the Spanish specimens, the ornament is mostly parallel to the edge of the carapace (ventrally, dorsally and posteriorly) and thus seem concentric, turning into reticulations in the centre of the posterior part of the carapace. This difference in ornament organization may be intraspecific or may represent a new species.

Occurrence. Upper Wenlock to at least the middle Ludlow series of France (Perrier et al. 2011); if the Spanish material is conspecific with *B. rugosa* the species range would extend into the late Pridoli.

Superfamily ENTOMOZOIDEA *sensu* ENTOMOZOACEA Přibyl, 1950

Family ENTOMOZOIDAE Přibyl, 1950

295 *Remarks*. Kozur (2004) changed the name Entomozoacea into Bouciacea n.nom. within the
296 Entomozocopina. Herein the concept of the 'Entomozoacea' is used in its widespread and
297 traditional sense, even though the type species of the type genus of the 'Entomozoidae',
298 namely Entomozoe tuberosa (Jones, 1861) from the Silurian of Scotland, is known to be an
299 entirely different form of ostracod (assigned to the myodocope superfamily Bolbozoacea
300 Bouček, 1936; see Siveter & Vannier 1990 for discussion and recommendations).
301
302 Genus ***Nudator*** Perrier, Siveter, Williams & Palmer, 2019
303
304 *Type species*. *Nudator inflatus* Perrier, Siveter, Williams & Palmer, 2019a, Ludlow Series,
305 Silurian, Wales.
306 *Other species*. *Nudator angiportatus* Perrier, Siveter, Williams & Palmer, 2019a, *Nudator*
307 *artumatus* Perrier, Siveter, Williams & Palmer, 2019a, *Nudator elegantulus* Perrier, Siveter,
308 Williams & Palmer, 2019b and *Nudator* sp. nov. A of Perrier et al., 2019a.
309 *Diagnosis*. Entomozoidae with bean-shaped to ovoid lateral outline, dorsal margin slightly
310 rounded. Adductorial sulcus narrow, well developed, extending up to ¾ of valve height.
311 Prominent postadductorial node present in type species only. Faint indentation in anterior
312 valve margin (Perrier et al. 2019a).
313 *Remarks*. *Nudator* differs from other entomozoid genera in having unornamented valves.
314 *Sineruga* and *Nudator* differ mainly in the valve outline in lateral view and in the positions of
315 tubercles.
316 *Stratigraphic and geographic range*. Homerian, Wenlock Series to Pridoli Series, Silurian
317 of England, Wales (Perrier et al. 2019a), Poland (Perrier et al. 2019b) and Spain; possibly also
318 present in the late Wenlock to upper Ludlow series of France (Perrier et al. 2019c).
319

320 ***Nudator angiportatus*** Perrier, Siveter, Williams & Palmer, 2019

321 Fig. 2G

322

323 2019a *Nudator angiportatus* sp. nov. - Perrier et al., pl. 14, figs 1-15.

324 2019b *Nudator angiportatus* Perrier, Siveter, Williams, and Palmer, 2019 - Perrier et al.,

325 fig. 2G, H.

326 2019c *Nudator angiportatus* Perrier et al., 2019a - Perrier et al., fig. 7N.

327

328 *Type material.* Holotype: a laterally compressed left valve (OUMNH 35267) figured by

329 Perrier et al. (2019a, pl. 14, figs 5-8, 14, 15).

330 *Type locality and horizon*. Long Mountain (loc. 56 of Perrier et al. 2019a), Wales; Lower

331 Irfon Formation, *Lobograptus scanicus* Biozone, Gorstian stage, Ludlow Series.

332 *Material and measurements* (mm). Six specimens from the shales of Mina Guillermín,

333 Spain; Pridoli, Silurian. Most complete specimen (Fig. 2G): L=1,47/H=1,19. Holotype:

334 L=2.70/H=2.35.

335 *Diagnosis*. Entomozoidae with bean-shaped to ovoid lateral outline, dorsal margin slightly

336 rounded. Adductorial sulcus narrow, well developed, extending up to ¾ of valve height. Faint

337 indentation in anterior valve margin (after Perrier et al. 2019a).

338 *Description*. Carapace bean-shaped in lateral outline. Greatest length around mid-height;

339 greatest height just in front of the adductorial sulcus. Valve outline in lateral view is slightly

340 concave dorsally, ventrally and posteriorly is evenly rounded, anteriorly above mid-height is

341 more sharply rounded, and anteriorly has a weak indentation. Valve surfaces gently inflated

342 overall, lacking distinct or discrete lobes. Adductorial sulcus narrow, occurs just in front of

343 mid-length and curves forward from dorsal margin to just below mid-height ending with the

344 adductor muscle spot. Anterior-anteroventral valve margin appears slightly concavely

345 indented in lateral view and has an apparent indentation. A simple elliptical adductor muscle
346 scar occurs at the slightly widened ventral extremity of the sulcus. Valves smooth.
347 *Remarks*. The Spanish material outline is slightly more rounded and the indentation more
348 pronounced than in the British specimens.
349 *Occurrence*. Upper Wenlock to Ludlow Series of Poland, Uzbekistan, Wales and England
350 and Pridoli Series of Spain. Possibly also present in the late Wenlock to upper Ludlow series
351 of France (Perrier et al. 2019c).
352
353 Genus ***Sineruga*** Perrier, 2012
354
355 *Type species*: *Sineruga insolita* Perrier, 2012; late Wenlock to early Pridoli Series,
356 Silurian, France.
357 *Other species*. *Sineruga* is currently regarded as monotypic.
358 *Diagnosis*. Entomozoidae with reniform outline, rounded to flattened anterior margin,
359 rounded ventral margin, slightly pointed posterior margin and straight dorsal margin. Anterior
360 half of valve less prominent than posterior. Sinusoidal adductorial sulcus with simple
361 elliptical adductor muscle spot. Valves connected above adductorial sulcus. In many cases a
362 tubercle is present ventrally and posterodorsally. Valves smooth (after Perrier 2012).
363 *Stratigraphic and geographic range*. Late Wenlock to Pridoli Series, Silurian of France
364 (Perrier 2012), England, Wales (Perrier et al. 2019a) and Spain.
365
366 ***Sineruga insolita*** Perrier, 2012
367 Fig. 2J
368
369 2012 *Sineruga insolita* sp. nov. - Perrier, pl. 14, figs 2-5, 7I, J, N.

2020 *Sineruga insolita* Perrier - Lorenzo et al., fig. 1V.

Type material. Holotype: a right valve preserved in 3D (FSL 710900) figured by Perrier (2012): figs. 2F, 3A). Paratype: a left valve preserved in 3D (FSL 710893) figured by Perrier (2012): fig. 2A.

Type locality and horizon. Les Chevrolières, St. Denis−d'Orques, Sarthe, France. Le Val Formation; uppermost Ludlow to lower Pridoli.

Material and measurements (mm). Three specimens from the shales of Mina Guillermín, Spain; Pridoli, Silurian. Most complete specimen (Fig. 2J): L=2,67/H=2,04. Holotype: L=2.91/H=1.75; Paratype: L=3.19/H=1.96.

Diagnosis. Same as genus.

Description. Reniform valves. Maximum valve length is across the posterior tubercle; maximum valve height at approximatively mid-length (ventral tubercle); maximum valve width across the centre of the posterior half of the carapace. Straight to gently curved dorsal margin. Anterodorsal part of valve flat, rounded to flattened in lateral outline, without rostrum or rostral incisure. Ventral margin evenly rounded. Two small tubercles are present in many specimens, situated posterodorsally and ventrally. Posterior margin slightly pointed with tubercle or rounded if tubercle lacking. Adductorial sulcus prominent, originates dorsally just before mid-length, is concave forward in its dorsal part, and ventrally is concave backward. A single reniform adductor muscle spot occurs at the inflection point of the sulcus. Valves smooth.

Remarks. Only three incomplete specimens of *Sineruga insolita* were recovered in the studied locality. However, the unique shape of sulcus, the position of the tubercles and the presence of the species in contemporaneous strata from the same region in Spain (Lorenzo et al. 2019) concur to the identification of *Sineruga insolita*.

Occurrence. Upper Wenlock to Pridoli Series of France (Perrier 2012) and Spain, and possibly England and Wales (Perrier et al. 2019a).

Genus ***Boucia*** Agnew, 1942

1936 *Basslerella* n. g. - Bouček, p. 60.

1942 *Boucia* n. subst. - Agnew, p. 757.

Type species. *Boucia ornatissima* (= *Basslerella ornatissima* Bouček, 1936; non *Basslerella* Kellett, 1935); Pridoli Series, Silurian of Czech Republic.

Other species. Boucia is currently regarded as monotypic.

Diagnosis. Entomozoidae with bean-shaped valves. Two sulci present: posteroventral sulcus curved and lightly marked; adductorial sulcus longer, deeper and showing the muscle spot near its ventral extremity. Ornament consist of densely arranged very thin ridges recalling the finger prints.

Remarks. The genus *Boucia* was created by Agnew (1942) in place of the invalid synonym name *Basslerella* Bouček, 1936 already used by Kellett (1935) for a different ostracod (*B. crassa* = Cytheridae, Pennsylvanian-Permian). Only one species was placed in this genus: *Boucia ornatissima.* Přibyl (1950) established a new sub-family (Bouciinae) for this genus and placed it within the Entomozoidae. Herein, we consider the erection this monotypic sub-family unnecessary and leave *Boucia* as a Genus within the Family Entomozoidae.

Stratigraphic and geographic range. Pridoli Series, Silurian of Czech Republic (Bouček 1936) and Spain.

Boucia ornatissima (Bouček, 1936)

Figs 4, 5

1936 *Basslerella ornatissima* n. sp. - Bouček, p. 61, pl. 6, fig. 1; text-fig. 3.

1950 *Boucia ornatissima* (Bouček) - Přibyl, p. 129, pl. 1, fig. 5.

1958 *Boucia ornatissima* (Bouček) - Pokorný, p. 315, text-fig. 1043.

1960 *Boucia ornatissima* (Bouček) - Zanina et Polenova, p. 442, text-fig. 837.

1988 *Boucia ornatissima* (Bouček, 1936) - Přibyl, p. 90, fig. 5.3; pl. 7, fig. 2.

2007 *Boucia ornatissima* (Bouček, 1936) - Perrier, p. 113, fig. 64.

2019c *Boucia ornatissima* (Bouček, 1936) - Perrier et al., p. 307, fig. 6.

Type material. Holotype: a right valve preserved in 3D (NM-L 14021) figured by Bouček (1936, text-fig 3a), Přibyl (1950, pl. 1, fig. 5), Přibyl (1988, fig. 5.3) and herein, Fig. 4F. Paratype: a left valve preserved in 3D (NM-L 14041) figured by Bouček (1936, text-fig 3b) and herein (Fig. 4E).

Type locality and horizon. Abandoned Quarry near Praha-Velká Chuchle village (Czech Republic); Pridoli (e2), Silurian.

Material and measurements (mm). Four specimens from the nodules of Mina Guillermín, Spain and 12 additional specimens from a small quarry near Praha-Velká Chuchle, Prague Basin, Czech Republic collected by V.P. in 2004 (= loc. 3 in Perrier et al. 2011, text-fig. 1B); Pridoli, Silurian. Most complete specimen from Spain (Fig. 4A-B), size range: L=1,65/H=1,01 to L=1,66/H=1,01. Holotype: L=1.75/H=1.05 (Fig. 4F); paratype: L=2.17/H=1.15 (Fig. 4E); new specimens from Czech Republic, size range: L=2,38/H=1,44 to L=2,59/H=1,55 (Fig. 4G-L).

Diagnosis. Same as genus.

444 *Description*. Carapace bean shaped and elongated; posterior and anterior margins convex;
445 ventral margin slightly convex; dorsal margin straight, even slightly concave at the level of
446 the adductorial sulcus. Anterodorsal part of the valve shows a slight depression followed by a
447 weak (eye?) tubercle just before the adductorial sulcus. No rostrum nor rostral incisure but a
448 slight indentation above the anteroventral depression. Adductorial sulcus situated in the
449 central part of the valve, appearing along the dorsal margin and curved frontward;
450 posteroventral sulcus originate near the dorsal connection in the posterior part of the carapace
451 and curves frontward almost reaching the ventral margin. Adductorial muscle spot small,
452 rounded or elliptical, situated near the extremity of the adductorial sulcus, another tiny
453 elliptical muscle spot situated slightly higher in the adductorial sulcus. Ornament consist of
454 very thin ridges and furrows, often bifurcated, recalling the finger prints; ridges thin, densely
455 packed and sub-vertical in the anterior and central part of the valve and broader and
456 concentric in the posterodorsal part of the carapace; ridges width around 10-15µm, furrows
457 around 20-25µm.
458 *Remarks*. *Boucia ornatissima* is very different from the other Silurian entomozoids as it
459 bears two sulci and has a unique fingerprint ornament. Morphologically, the closest species
460 with vertical ribbing pattern is the younger *Monosulcoentomozoe monosulcata* Wang, 1989
461 from the Early Devonian (late Lochkovian to Pragian) of China; it differs from *Boucia* in
462 having only one sulcus. The Chinese Early Devonian *Trisulcoentomozoe* Wang, 1989 differs
463 in the ribbing pattern and by having a very unusual third sulcus. *Bisulcoentomozoe*
464 *tuberculata* Wang & Zang, 1983 (fig. 2-3, pl. 2, fig. 5-9) from the Early to Middle Devonian
465 of Guangxi Province, China bears a fine ornament close to that of *B. ornatissima*, but has a
466 shallow anteroventral sulcus. In addition, *B. tuberculata* displays a posterodorsal spine and
467 the disposition of its ornament is quite different (i.e. sub-horizontal for *Bisulcoentomozoe* and
468 sub-vertical for *Boucia*). The holotype of *Bisulcoentomozoe tuberculata* Wang and Zang,

1983 was refigured by Groos-Uffenorde and Rabien (2014, fig. 5a) and compared with *Entomis* (*Richeria*) n.sp. (aff. *torta*) Kegel 1934 from the Early Devonian of the northern Harz Mountain, Germany. The other *Bisulcoentomozoe* species described by Wang and Zang (1983), *B.*? *kurtis* (pl. 1, fig. 15-17) and *B.*? sp. 1 (pl. 3, fig. 8-9), are also different from *B. ornatissima* (organization of the ornament and sulcus shape). Because of the resemblances between the Czech and Chinese species we favour the interpretation that part of the Devonian entomozoids may derive from *B. ornatissima*, one of the evolution possibilities shown in fig. 2 of Groos-Uffenorde et al. (2000, p. 102).

Occurrence. Late Pridoli Series, Silurian of Czech Republic and Spain.

Superfamily CYPRIDINOIDEA *sensu* CYPRIDINACEA Baird, 1850

Family CYPRIDINIDAE Baird, 1850

Genus ***Silurocypridina*** Perrier, Vannier & Siveter, 2011

Type species. *Silurocypridina retroreticulata* Perrier, Vannier & Siveter, 2011 from the Silurian of France.

Other species. *Silurocypridina variostriata* Perrier, Vannier & Siveter, 2011 and *Silurocypridina calva* Perrier, Vannier & Siveter, 2011.

Diagnosis. Cypridinidae with valves broadly ovoid in lateral outline and a gently dome-like relief. Anterodorsal part of the carapace inflated in some 3D specimens. Rostrum and rostral incisure well developed, rostrum protrudes well beyond anterior valve margin. Adductor muscle scar small, subcentral, generally crescent-shaped. Valves are smooth anterodorsally and mostly reticulate or corrugate elsewhere or entirely smooth (modified after Perrier et al. 2011).

494 *Remarks*. The Spanish specimens of *Silurocypridina* show a slightly inflated anterodorsal
495 part of their carapaces just above the rostrum and the rostral incisure (see e.g. Fig. 6E). This
496 feature, which may be related to vision (eye tubercle?), is not visible on flattened specimens.
497 Although it was not noted by previous studies it is probably present in other *S. calva* 3D
498 specimens such as those from France and Sardinia (see Perrier et al. 2011, pl. 5, figs 8-11).
499 *Stratigraphic and geographic range*. Upper Wenlock to Pridoli Series, Silurian of Czech
500 Republic (Perrier et al. 2011), France (Perrier et al. 2011), Sardinia (Gnoli et al. 2009), Wales
501 and England (Perrier et al. 2019a), Poland (Perrier et al. 2019b), Uzbekistan (Mikhailova et al.
502 2020) and Spain.
503
504 ***Silurocypridina calva*** Perrier, Vannier & Siveter, 2011
505 Figs 2D-F, 6
506
507 2019a *Silurocypridina calva* Perrier, Vannier & Siveter, 2011 - Perrier et al. pl. 17, figs 1-
508 5, 8-11 (see p. 49 for full synonymy).
509 2019b *Silurocypridina calva* Perrier et al., 2011 - Perrier et al., fig. 2L.
510 2019c *Silurocypridina calva* Perrier et al., 2011 - Perrier et al., fig. 7T.
511 2020 *Silurocypridina calva* Perrier, Vannier & Siveter - Lorenzo et al., fig. 1U.
512 2020 *Silurocypridina calva* Perrier et al., 2011 - Mikhailova et al., fig. 2J, K; fig. 3D, H, L,
513 P, T.
514 2021 *Silurocypridina calva* Perrier et al., 2011 - Mikhailova and Siveter, fig. 11p.
515
516 *Type material*. Holotype: a three-dimensionally preserved left valve (LPB 18926) figured
517 by Perrier *et al.* (2011, pl. 5, figs 8, 9).

518 *Type locality and horizon*. Les Chevrolières, St. Denis-d'Orques, Sarthe, France. Le Val
519 Formation; uppermost Ludlow to lower Pridoli.
520 *Material and measurements* (mm). 374 specimens from the shales (124 specimens) and the
521 nodules (250 specimens) of Mina Guillermín, Spain; Pridoli, Silurian. Size range:
522 L=1,05/H=0,87 to L=3,66/H=3,12. Holotype: L=2,38/H=1.48.
523 *Diagnosis*. *Silurocypridina* with unornamented valves.
524 *Description*. Valve dome-like, with sub-ovoid lateral outline; hinge short. Rostrum well
525 developed, representing 10–20% of valve length, protruding distinctly forward beyond
526 anteroventral margin of valve. Anterodorsal part of the carapace inflated in some 3D
527 specimens. Rostral incisure well developed, rounded to angular in lateral outline. Adductor
528 muscle scar small, subcentral, crescent-shaped and convex anteriorly. Valves smooth. During
529 ontogeny valve shape changes from almost circular to sub-ovoid.
530 *Remarks*. The cosmopolitan species *S. calva* displays considerable variation in valve
531 outline and rostrum shape, especially when comparing 3D and flattened specimens from
532 different localities.
533 *Occurrence*. Upper Wenlock to Pridoli series of Czech Republic, France, Poland, Wales,
534 England, Uzbekistan, Spain and possibly Sardinia (see Perrier et al. 2011, 2019a-c for
535 references).
536
537 ***Silurocypridina variostriata*** Perrier, Vannier & Siveter, 2011
538 Fig. 2H, I
539
540 2011 *Silurocypridina variostriata* sp. nov. - Perrier et al., p. 1386, pl. 4, figs 8-16, text-figs
541 6, 8A, 9I
542 2022 *Silurocypridina variostriata* Perrier *et al.* 2011 - Siveter et al., pl 1. fig. o.

543

544 *Type material*. Holotype: flattened right valve, FSL 710480a figured by Perrier *et al.* 2011:
545 pl. 4, fig. 10.

546 *Type locality and horizon*. Les Buardières, Mayenne, France (locality 7 of Perrier et al.
547 2011); upper Wenlock to middle Ludlow series.

548 *Material and measurements* (mm). 25 specimens from the shales of la Mina Guillermín,
549 Spain; Pridoli, Silurian. Size range: L=3,00/H=2,49 to L=4,17/H=3,20. Holotype:
550 L=4,08/H=2,80.

551 *Diagnosis*. *Silurocypridina* species with corrugate valve ornament.

552 *Description*. Carapace with subovoid lateral outline; hinge short. Rostrum well developed,
553 long, representing c.a. 20% of valve length, protruding prominently anteriorly in front of
554 anteroventral margin of valve. Rostral incisure well developed, wide and generally rounded in
555 lateral outline. Adductor muscle scar small, subcentral, crescent-shaped and convex
556 anteriorly. Posterior and ventral part of valves are corrugated, with series of fine, sinuous and
557 bifurcated ridges that are sub-vertical across centre of valve, curved backward ventrally and
558 becoming more horizontal in the posterior half of the carapace. Both ridges and intervening
559 grooves are 50–100 µm wide. Ridges converge to form a well-developed ridge along ventral
560 margin of the valve. Ornament is absent in anterodorsal part of valves (less than 20% of
561 lateral valve area).

562 *Remarks*. This is the first occurrence of *S. variostriata* outside France. The Spanish
563 material differ slightly from the French one in the organization of the ornament.

564 *Occurrence*. Upper Wenlock to Pridoli Series of France (see Perrier *et al*. 2011) and Spain.

565

566

567 Genus ***Calocaria*** Vannier, 1987

568

569 *Type species*. *Calocaria maurae* Vannier, 1987, from the Silurian of Morocco.

570 *Other species*. *Calocaria robusta* Perrier et al., 2011 and *Calocaria callundosa* sp. nov.

571 *Diagnosis*. Cypridinidae with subcircular to ovoid valve outline. Well-developed rostrum
572 and rostral incisure protruding beyond anteroventral valve margin. Adductor muscle scar
573 small, subcentral, crescent-shaped, convex anteriorly. Most of valve surface is corrugated,
574 consisting of sinuous and bifurcated sub-vertical to sub-horizontal ridges. In the type species,
575 the corrugation transforms posteriorly into more or less coalescent tubercles. Ornament absent
576 in the inflated anterodorsal part of the valves (after Perrier et al. 2011).

577 *Remarks*. *Calocaria* species differ from *Silurocypridina* by a smaller size, a generally more
578 rounded outline and a more prominently inflated anterodorsal part of the valves (see Fig. 7B,
579 8A, 9F). This inflated anterodorsal part of the valves may be related to vision (possibly being
580 the site of the lateral eyes) and strongly resembles that of Cypridinelliformidae such as the
581 Devonian *Cypridella ortelii* (see Becker and Bless, 1987) or the Permian *Cypridinelliforma*
582 *rex* (see Kornicker and Sohn, 2000).

583 *Stratigraphic and geographic range*. Wenlock (-Ludlow?) Series of Morocco (Vannier
584 1987) and Pridoli Series of France (Perrier et al. 2011) and Spain.

585

586 ***Calocaria maurae*** Vannier, 1987

587 Fig. 7

588

589 1987 *Calocaria maurae* sp. nov. - Vannier, p. 45-48, pl. 14

590

591 *Type material*. Holotype: a flattened right valve, IGR 33100 figured by Vannier 1987: pl.
592 14, 46, figs 1-3.
593 *Type locality and horizon*. Siltstones and mudstones (Wenlock - Ludlow?) in the
594 Talmakent section near Talmakent, High-Atlas, Morocco (Vannier 1987).
595 *Material and measurements* (mm). 85 specimens from the nodules of Mina Guillermín,
596 Spain; Pridoli, Silurian. Size range: L=2,20/H=1,72 to L=3,25/H=2,44. Holotype:
597 L=3,05/H=2,61.
598 *Diagnosis*. *Calocaria* with corrugation transforming posteriorly into more or less
599 coalescent tubercles.
600 *Description*. Valve with sub-circular outline; length slightly greater than height. Rostrum
601 well developed and protruding anteriorly from rest of valve in lateral outline. Rostral incisure
602 well developed, with curved outline. Adductor muscle scar subcentral, small, vaguely
603 crescent shaped, convex anteriorly. Most of valve surface covered with corrugations,
604 consisting of sub-vertical ridges anteriorly, curving posteriorly to become sub-horizontal and
605 transforming into more or less coalescent tubercles. Ridges are 100-200 µm wide, separated
606 by 100-300 µm wide grooves. More or less individualised tubercles diameter varies from 100-
607 300 µm. The posterior ornament appears to swirl away from the region of the adductor
608 muscle scar. Ornament absent in the inflated anterodorsal part of the valves (c.a. 15% of
609 lateral valve area).
610 *Remarks*. *C. maurae* differs from other *Calocaria* species by its partly tuberculate
611 ornament.
612 *Occurrence*. Wenlock – (Ludlow?) Series of Morocco (Vannier 1987) and Pridoli series of
613 Spain.
614
615 ***Calocaria robusta*** Perrier, Vannier & Siveter, 2011

Fig. 8

2011 *Calocaria robusta* sp. nov. - Perrier *et al.*, p. 1388, pl. 5, figs 15–17, 20, 21; text-figs 6, 8A. Non pl. 5, figs 18, 19 (= *C. callundosa* sp. nov.)

Type material. Holotype: a flattened left valve, FSL 710684 figured by Perrier *et al.* 2011: pl. 5, fig. 21.

Type locality and horizon. Saint-Sauveur-le-Vicomte, Manche, France (locality 11 of Perrier et al. 2011); lower Pridoli Series.

Material and measurements (mm). 92 specimens from the nodules of Mina Guillermín, Spain; Pridoli, Silurian. Size range: L=1,73/H=1,54 to L=3,04/H=2,42. Holotype: L=2,12/H=1,65.

Diagnosis. *Calocaria* with strongly marked ornament (12-18 ridges); ridges widening toward posterior end and abruptly ending before posterior margin.

Description. Valve with sub-circular outline; length slightly greater than height. Rostrum well developed and slightly protruding anteriorly from rest of valve in lateral outline. Rostral incisure well developed, with curved outline. Adductor muscle scar subcentral, small, vaguely crescent shaped, convex anteriorly. Most of valve surface covered with strongly marked corrugations (12-18 ridges), consisting of sub-vertical ridges anteriorly, curving posteriorly to become sub-horizontal. Ridges widening toward posterior end and abruptly ending before posterior margin. Ridges are 100 µm wide, separated by 200-300 µm wide grooves. The posterior ornament appears to swirl away from the region of the adductor muscle scar; the first 2-3 anteroventral ridges converge to form a single ridge along ventral margin of the valve. Ornament absent in the inflated anterodorsal part of the valves (c.a. 15% of lateral valve area).

641 *Remarks*. *C. robusta* differs from *C. maurae* by the absence of tuberculate ornament and
642 from *C. callundosa* sp. nov by it ornament consisting of fewer (12-18 *vs* 22-26 respectively)
643 and more strongly marked ridges and furrows.
644 *Occurrence*. Pridoli Series of France (Perrier et al. 2011) and Spain.
645
646 ***Calocaria callundosa*** Perrier, sp. nov.
647 Fig. 9
648
649 2011 *Calocaria robusta* sp. nov. - Perrier *et al.*, pl. 5, figs 18, 19
650
651 *Derivation of name.* From latin *callus* 'hard skin' and *undosus* 'billowy, full of waves'
652 alluding to the external ornament of the carapace.
653 *Type material*. A slightly flattened right valve, MGM-8071S; Fig. 9A-B.
654 *Type locality and horizon*. Alcaracejos (Córdoba, Spain), Mina Guillermín section; Pridoli
655 Series.
656 *Material and measurements* (mm). 22 specimens from the nodules of Mina Guillermín,
657 Spain; Pridoli, Silurian. Size range: L=1,93/H=1,45 to L=3,09/H=2,38. Holotype:
658 L=2,24/H=1,65.
659 *Diagnosis*. *Calocaria* with densely packed, faint, ridges and furrows (22-26 ridges).
660 *Description*. Valve with sub-circular to ovoid outline; length slightly greater than height.
661 Rostrum well developed and protruding anteriorly from rest of valve in lateral outline. Rostral
662 incisure well developed, with curved outline. Adductor muscle scar subcentral, small, vaguely
663 crescent shaped, convex anteriorly. Most of valve surface covered with faintly marked
664 corrugations (22-26 ridges), consisting of sub-vertical ridges anteriorly, curving posteriorly to
665 become sub-horizontal. Ridges are 100 µm wide, separated by 50-100 µm wide grooves. The

posterior ornament appears to swirl away from the region of the adductor muscle scar; the first 2-3 anteroventral ridges converge to form a single ridge along ventral margin of the valve. Ornament absent in the inflated anterodorsal part of the valves (c.a. 15% of lateral valve area).

Remarks. *C. callundosa* sp. nov. differs from *C. maurae* Vannier, 1987 by the absence of tuberculate ornament and from *C. robusta* Perrier et al., 2011 by its ornament consisting of more numerous (22-26 *vs* 12-18 respectively) and less marked ridges and furrows. Two of the *Calocaria* specimens figured by Perrier et al. (2011) are herein placed within *C. callundosa* sp. nov. based on their densely packed and faint corrugations.

Occurrence. Pridoli Series of France (Perrier et al. 2011) and Spain.

5. Discussion

5.1. Shales and nodules ostracod assemblages from Mina Guillermín

With 954 specimens belonging to ten species, the Spanish fauna is by far the most diverse myodocope fauna known during the Pridoli. However, when looking into the details of Mina Guillermín fauna, two different assemblages (shales *vs* nodules), with different species composition, can be identified (Fig. 10).

The shales assemblage consists of 438 specimens belonging to five species: *B. anomala* (280 spec.), *S. calva* (124 spec.), *S. variostriata* (25 spec.), *N. angiportatus* (6 spec.) and *S. insolita* (3 spec.). Two species, *B. anomala* and *S. calva*, represent more than 90% of this assemblage. Apart from *S. variostriata*, all the species in the shales assemblage have already been recorded in Pridoli strata.

690 The nodules assemblage consists of 516 specimens belonging to seven species: *S. calva*
691 (250 spec.), *C. robusta* (92 spec.), *C. maurae* (85 spec.), *B. anomala* (58 spec.), *C. callundosa*
692 sp. nov. (22 spec.), *B.* aff. *rugosa* (5 spec.) and *B. ornatissima* (4 spec.). Four species
693 dominate this assemblage: *S. calva*, *C. robusta*, *C. maurae* and *B. anomala*. Apart from *C.*
694 *maurae*, *C. callundosa* sp. nov. and *B.* aff. *rugosa*, all the species in the nodules assemblage
695 have already been recorded in Pridoli strata.
696 Only the two most abundant species are present both in shales and nodules: *B. anomala*
697 which dominate the shale assemblage (63,9% of spec.) and *S. calva* which dominate the
698 nodule assemblage (48,4% of spec.). When looking at the size of the specimens of these two
699 species, it appears that both juvenile and adults of *B. anomala* are present in the shales and the
700 nodules, while it is not the case for *S. calva* for which only small specimens have been
701 recovered in the nodules and bigger ones in the shales (Fig. 11).
702 Several hypotheses can explain the discrepancies between these two assemblages:
703
704 *5.1.1. Sampling bias.*
705 Although we did our best to collect specimens from nodules and shales in the same
706 horizon, it is still possible that these two lithologies are not exactly contemporaneous. As the
707 shales are highly tectonised in this area, it is imaginable that our specimens could be a few
708 centimetres or decimetres apart stratigraphically. Even if it is very difficult to evaluate time of
709 deposition in such context, these few centimetres or decimetres could easily represent several
710 thousand or tens of thousands of years. If this is the case, we would be dealing with two
711 different faunas of slightly different ages that succeeded in time in the same area.
712
713 *5.1.2. Taphonomic bias.*

We could also be facing a taphonomic bias related to the different preservation pathways of nodules and shales. The formation of the nodules was probably triggered by the decaying remains of *Scyphocrinites* thus creating a microenvironment in its surrounding (Raiswell and Fisher 2000; Yoshida et al. 2018). This chemically different microenvironment could have affected, in an unknown way, the preservation of the ostracod valves thus allowing the preservation of different taxa or different valve sizes in distinct environmental conditions.

5.1.3. Different ecologies.

These two assemblages could also reflect two different faunas with distinct ecologies. The vast majority of Silurian myodocopes are recovered in rocks such as black shales, siltstones and mudstones (see e.g. Perrier et al. 2019c). They are interpreted as being planktonic, living in the open ocean in the pelagic environment (Siveter et al. 1991; Perrier et al. 2015). Based on the same lines of evidence (depositional setting, associated fauna, functional morphology and palaeogeographic distribution, see Siveter et al. 1991), it would also be the case for the shale assemblage of Mina Guillermín. Thus, the nodules assemblage may not represent the 'background planktonic fauna', but possibly a specific assemblage associated with living or dead *Scyphocrinites*.

Since Haude (1972) demonstrated that the loboliths of *Scyphocrinites* are buoy structures, this genus is widely accepted as a, possibly mid-water, pelagic floater (e.g. Hess 1999; Seilacher and Hauff 2004). As it was probably the case for pseudoplanktonic crinoid such as the Holzmaden crinoid raft colonies (Hunter et al. 2020), the *Scyphocrinites* colonies would probably have attracted a wide range animals searching for food or refuge (Carlton et al. 2017). It is possible that the nodules ostracod assemblage represents free swimming species that lived in close association or around the *Scyphocrinites* colonies (Fig. 12) and thus were fossilized with them in the nodules. These species could have fed either on the crinoid itself

739 or on the crinoid's food. In the case of *Silurocypridina calva*, the floating crinoid may have
740 acted as a 'nursery' for juveniles, which could explain the peculiar size discrepancies of this
741 species specimens in the shales and in the nodules.
742 Another explanation for this peculiar association could be that the ostracods were
743 scavenging on the decaying crinoids once they reached the sea floor after their death.
744 Scavenging is a frequent feeding behaviour in Recent nektobenthonic cypridinid myodocopes
745 (e.g. Vannier et al. 1998). This feeding strategy was also proposed in the fossil record for
746 association of myodocopes with cephalopods (Gabbott et al. 2003; Perrier et al. 2011;
747 Weitschat 1983) and shark remains (Wilkinson et al. 2004; Wilby et al. 2005). If this is the
748 case, the nodules myodocope assemblage would consist of either nektobenthonic or demersal
749 species living close to the sea floor. This would be in contradiction with the absence of
750 benthonic species (except for one bivalve species, *Panenka* sp.; Lorenzo Álvarez 2015) at this
751 locality, possibly indicating a sea floor improper to benthonic life, and with the transoceanic
752 distribution of several of these myodocopes species (e.g. *B. anomala* and *S. calva*; see Perrier
753 et al. 2019c).
754
755 ***5.2. Temporal and palaeogeographical distributions***
756
757 Pridoli myodocope ostracods are scarce in the fossil record. They have only been
758 recovered in the Czech Republic (*B. ornatissima* and possibly *B. anomala*, *N. angiportatus*
759 and *Rhomboentomozoe rhomboidea*), France (*S. insolita*, *C. robusta*, *C. callundosa* sp. nov.
760 and possibly *B. anomala* and *S. calva*) and Sardinia (*B. anomala*, *Parabolbozoe bohemica, N.*
761 *angiportatus*, *Richteria migrans* and *S. calva*; Fig. 13A; see details and references in Perrier et
762 al. 2019c).

763 *Calocaria maurae* is only known from poorly dated (Wenlock or Ludlow?) strata of
764 Morocco (Vannier 1987). *S. variostriata* and *B. rugosa* latest occurrence were in middle
765 Gorstian strata (*Lobograptus scanicus* Biozone) of France. *B. anomala*, *S. calva* and *N.*
766 *angiportatus* were only known with certainty from the lowermost Pridoli strata (*Skalograptus*
767 *parultimus* Biozone) of the Czech Republic, France and Sardinia. *S. insolita*, *C. robusta* and
768 *C. callundosa* sp. nov. uppermost occurrences reached the end of the *S. parultimus-ultimus*
769 Biozones in France. *B. ornatissima* was already known within the ?*Wolynograptus bouceki* -
770 *S. transgrediens* Biozones of the Czech Republic. The new findings in Mina Guillermín
771 extend the temporal distribution of all these myodocope species to the uppermost Pridoli (?*W.*
772 *bouceki* - *S. transgrediens* Biozones; Fig. 13A). These new occurrences raise the question of
773 the temporal extension of some these myodocope species. For example, *B. anomala* and *N.*
774 *angiportatus* are now known from the base of the Homerian (i.e. middle part of the Wenlock
775 stage) till the latest Pridoli, which represents a time interval of more than 20 My. The fact that
776 most of these long-ranging species bear few diagnostic characters (e.g. simple adductorial
777 muscle scars, unornamented carapaces) and show some small morphological variations
778 through time may indicate a cluster of morphologically similar species.
779 All the Pridoli myodocope ostracod records are situated on a small area of the North
780 Gondwanan margin around 30°S of latitude. The most distant outcrops are the Spanish and
781 Czech ones separated by, at most, a few 1000s of km (Fig. 13B). This pattern strongly
782 contrasts with that of Ludlow myodocopes species which clearly have a transoceanic
783 distribution (see Perrier et al. 2019c). This Pridoli palaeogeographic range restricted to
784 European countries possibly reflects a sampling bias, the species only being known in areas
785 extensively mapped and sampled for fossils. Though we cannot rule out the possibility of
786 such faunas not being preserved or not being present for various reasons, another explanation
787 for this restricted distribution could be linked to changes in the environments of older

myodocope bearing localities. For example, the UK, which bear the most diverse myodocope fauna for the mid Silurian (20 species; Perrier et al. 2019a), sees its depositional environment changing from open marine settings during the Ludlow, to shallow marine or even continental settings during the Pridoli.

6. Conclusion.

We describe herein, two distinct myodocope ostracod faunas from the same horizon (late Pridoli, possibly ?*Wolynograptus bouceki - Skalograptus transgrediens* Biozones) of Mina Guillermín (Alcaracejos, province of Córdoba, southern Spain).

- The fauna recovered in the black shales, comprises five species (by abundance: *B. anomala*, *S. calva*, *S. variostriata, N. angiportatus* and *S. insolita*) belonging to three myodocope families (bolbozoids, entomozoids and cypridinids).

- The fauna recovered in the large dark-reddish calcareous nodules and associated with the planktonic crinoid *Scyphocrinites elegans*, comprises seven myodocope species including one new to science (by abundance: *S. calva*, *C. robusta*, *C. maurae*, *B. anomala*, *C. callundosa* sp. nov., *B.* aff. *rugosa* and *B. ornatissima*).

Although the shales and nodules faunas have two species in common (*B. anomala* and *S. calva*), they are clearly different in terms of diversity, abundances and size of the specimens. The discrepancies between these two assemblages could either be explained by sampling (not exactly the same horizon) or taphonomic (microenvironment related to the decaying remains of *Scyphocrinites*) bias, or because they represent faunas with different ecologies. If the latter hypothesis is true, the myodocope fauna in the shales could represent the 'background' planktonic fauna, while the fauna in the nodules could have lived either in the water column

812 in the vicinity of the *Scyphocrinites* 'floating islands', or on the sea floor, scavenging around
813 the dead crinoids.
814 With ten species, the Spanish fauna is by far the most diverse myodocope fauna known
815 during the Pridoli. Among these ten species, four (*S. variostriata, C. maurae*, *C. callundosa*
816 sp. nov. and *B.* aff. *rugosa*) are recorded in Pridoli strata for the first time. All the Pridoli
817 myodocope ostracod records are situated on a small area of the North Gondwanan margin
818 around 30°S of latitude. This peculiar restricted palaeogeographic distribution possibly
819 reflects a sampling bias around European countries, the species only being known in areas
820 extensively mapped and sampled for fossils.
821
822 **Acknowledgements**
823 This paper is a contribution to project PDI2021-125585NB-100 of the Spanish Ministry of
824 Science and Innovation (to JCG-M and SL). Palaeontological sampling was made by JCG-M in
825 the frame of a collaboration contract with the IGME-Andalusian Government for producing the
826 Mapa Geológico Continuo Digital to 1:200,000 scale of part of the province of Córdoba. We
827 thank Martina Nohejlová (Czech Geological Survey, Czeck Republic) and Lenka Váchová
828 (National Museum, Prague, Czeck Republic) for providing photographs of the type specimens
829 of *Boucia ornatissima*.
830
831 **References**
832 Agnew, A.F., 1942. Bibliographic index of new genera and families of Paleozoic Ostracoda
833 since 1934. Journal of Paleontology 16, 756-763.
834 Apalategui Isasa, O., Higueras Higueras, P., Pérez Lorente, F., Roldán García, F.J., 1985. Mapa
835 y Memoria explicativa de la Hoja nº 880 (Espiel) del Mapa Geológico de España a escala
836 1:50.000 (Segunda Serie). Instituto Geológico y Minero de España, Madrid, 58 pp.

837 Aragonés-Illanas, P., 2015. Conodontos del Silúrico del Dominio Obejo-Valsequillo (suroeste
838 del Macizo Ibérico). TFM Paleontología Avanzada, Universidad Complutense de Madrid, 43
839 p. (unpublished). [In Spanish].
840 Arenas, R., Díez Fernández, R., Rubio Pascual, F.J., Sánchez Martínez, S., Martín Parra, L.M.,
841 Matas, J., González del Tánago, J., Jiménez-Díaz, A., Fuenlabrada, J.M., Andonaegui, P.,
842 García-Casco, A., 2016. The Galicia–Ossa-Morena Zone: Proposal for a new zone of the
843 Iberian Massif. Variscan implications. Tectonophysics 681, 135-143.
844 Baird, W., 1850. The Natural History of the British Entomostraca. The Ray Society, London,
845 364 pp.
846 Barrande, J., 1872. Système Silurien du Centre de la Bohême, Volume 1 Supplement. Prague-
847 Paris, 647pp. [In French].
848 Bassler, R.S., Kellet, B., 1934. Bibliographic index of Paleozoic Ostracoda. Geological
849 Society of America, Special Papers 1, Washington, 500pp.
850 Becker, G., Bless, M.J.M., 1987. Cypridinellidae (Ostracoda) aus dem Oberdevon Hessens.
851 Geologisches Jahrbuch Hessen 115, 29-56. [In German].
852 Bouček, B., 1936. Die Ostracoden des böhmischen Ludlows (Stufe eβ). Neues Jahrbuch für
853 Mineralogie, Geologie und Paläontologie, Abteilung B 76 (1), 31-98. [In German].
854 Carlton, J.T., Chapman, J.W., Geller, J.B., Miller, J.A., Carlton, D.A., McCuller, M.I.,
855 Treneman, N.C., Steves, B.P., Ruiz, G.M. 2017. Tsunami-driven rafting: transoceanic
856 species dispersal and implications for marine biogeography. Science 357, 1402–1406.
857 Dalloni, M., 1930. Étude géologique des Pyrénées catalanes. Annales de la Faculté des
858 Sciences de Marseille 26, 1-373. [In French].
859 Dégardin, J.M., Lethiers, F., 1982. Une microfaune (Conodonta, Ostracoda) dans le Silurien
860 terminal des Pyrénées centrales espagnoles. Revista Española de Micropaleontología 14,
861 335-358. [In French].

862 Delgado, J.F.N., 1908. Système Silurique du Portugal. Étude de stratigraphie paléontologique.
863 Memoires de la Commission du Service Géologique du Portugal, Lisboa, 245 pp. [In
864 French].
865 Díez Fernández, R., Arenas, R., 2015. The Late Devonian Variscan suture of the Iberian
866 Massif: A correlation of high-pressure belts in NW and SW Iberia. Tectonophysics 654,
867 96-100.
868 Díez Fernández, R., Arenas, R., Pereira, M.F., Sánchez-Martínez, S., Albert, R., Martín Parra,
869 L.M., Rubio Pascual, F.J., Matas, J., 2016. Tectonic evolution of Variscan Iberia:
870 Gondwana-Laurussia collision revisited. Earth-Science Reviews 162, 269-292.
871 Gabbott, S., Siveter, D.J., Aldridge, R., Theron, J., 2003. The earliest myodocopes: ostracodes
872 from the late Ordovician Soom Shale Lagerstätte of South Africa. Lethaia 36(3), 151-160.
873 Gnoli, M., Perrier, V., Serventi, P., 2009. The state of research on Sardinian Silurian
874 Crustacea. In: Corradini, C., Ferretti, A., Štorch, P. (Eds): The Silurian of Sardinia.
875 Rendiconti della Societa Paleontologica Italiana 3 (1), 143-155.
876 Groos-Uffenorde, H., Lethiers, F., Blumenstengel, H. 2000. Ostracodes and Devonian
877 Stratigraphy. Courier Forschungs-Institut Senckenberg, 220, 99-111.
878 Groos-Uffenorde, H., Rabien, A., 2014. Zur Verbreitung pelagischer Ostracoden im Devon
879 Deutschlands. Geologisches Jahrbuch Hessen, 138, 37-47. [In German].
880 Gutiérrez-Marco, J.C., Sarmiento, G.N., Rábano, I., 2014. Un olistostroma con cantos y
881 bloques del Paleozoico Inferior en la cuenca carbonífera del Guadalmellato (Córdoba).
882 Parte 2: Bioestratigrafía y afinidades paleogeográficas. Revista de la Sociedad Geológica
883 de España 27 (1), 27-45. [In Spanish].
884 Gutiérrez-Marco, J.C., Sarmiento, G.N., Robardet, M., Rábano, I., Vaněk, J., 2001. Upper
885 Silurian fossils of Bohemian type from NW Spain and their palaeogeographical interest.
886 Journal of the Czech Geological Society 46 (3-4), 247-258.

887 Haude, R., 1972, Bau und Funktion der *Scyphocrinites*-Lobolithen. Lethaia, 5, 95–125. [In
888 German].
889 Hess, H., 1999. Scyphocrinitids from the Silurian–Devonian boundary of Morocco. In: Hess,
890 H., Ausich, W.I., Brett, C.E., Simms, M.J. (Eds), Fossil Crinoids. Cambridge University
891 Press, 93-102.
892 Hunter, A.W., Casenove, D., Mayers, C., Mitchell, E.G., 2020. Reconstructing the ecology of
893 a Jurassic pseudoplanktonic raft colony. Royal Society Open Science, 7(7), 200142.
894 Kegel, W., 1934. Zur Kenntnis paläozoischer Ostracoden 4. Über die Gattung Entomis und
895 ihre mittel-devonischen Arten. Jahrbuch der preußischen geologischen Landesanstalt zu
896 Berlin for 1933, 54, 409-20. [In German].
897 Kellett, B., 1935. Ostracodes of the Upper Pennsylvanian and the Lower Permian strata of
898 Kansas: III. Bairdiidae (concluded), Cytherellidae, Cypridinidae, Entomoconchidae,
899 Cytheridae and Cypridae. Journal of Paleontology 9, 132-166.
900 Kornicker, L.S., Sohn, I.G., 2000. Myodocopid Ostracoda from the Late Permian of Greece
901 and a basic classification for Paleozoic and Mesozoic Myodocopida. Smithsonian
902 Contributions to Paleobiology 91, 1-33.
903 Kozur, H., 2004. Pelagic uppermost Permian and the Permian Triassic boundary conodonts of
904 Iran, part 1: taxonomy. Hallesches Jahrbuch für Geowissenschaften, 39-68.
905 Kříž, J., 1992 Silurian Field Excursions: Prague basin (Barrandian), Bohemia. National
906 Museum of Wales Geological series, Cardiff, 13, 111 pp.
907 Latreille, P.A., 1802. Histoire naturelle générale et particulière des Crustacés et des Insectes,
908 Familles naturelles des genres, Third edition. Dupuis, Paris, 467 pp. [In French].
909 Lorenzo Álvarez, S., 2015. Bioestratigrafía del Silúrico de la Zona Centroibérica meridional
910 (España). Tesis Doctoral, Univ. Complutense de Madrid. 435+170 pp. (unpublished). [In
911 Spanish].

912 Lorenzo, S., Gutiérrez-Marco, J.C., Perrier, V., Serventi P., 2020. Yacimientos
913 paleontológicos del Silúrico superior de Hinojosa del Duque (provincia de Córdoba,
914 Dominio de Obejo-Valsequillo, suroeste de España). Geogaceta, 67, 75-78. [In Spanish].
915 Manda, Š., Slavík, L., Štorch, P., Tasáryová, Z., Čáp, P., 2023. Division of Přídolí Series in
916 Central Bohemia: graptolite and conodont biostratigraphy, faunal changes, and
917 geochemical record. Newsletters on Stratigraphy, 56, 89-123.
918 Mikhailova, E.D., Perrier, V., Williams, M., Siveter, D.J., Tarasenko, A., Salimova, F., Kim,
919 I.A., 2020. Cosmopolitan myodocope ostracods from the Silurian of Uzbekistan, Central
920 Asia. Bulletin de la Société Géologique de France 191(1).
921 Mikhailova, E.D., Siveter, D.J., 2021. Endemic Silurian ostracod faunas of the Southern Tien
922 Shan, Central Asia. Marine Micropaleontology 164, 101969.
923 Palacios, T., Eguíluz, L., Apalategui, O., Jensen, S., Martínez-Torres, L.M., Carracedo, M.,
924 Gil-Ibarguchi, J.I., Sarrionaindia, F., Martí, M., 2013. Mapa Geológico de Extremadura
925 1/350.000 y Memoria. Servicio Editorial de la Universidad del País Vasco, Bilbao, 222 pp.
926 Perrier, V., 2007. Biodiversité et écologie des ostracodes myodocopes (Crustacea) du Silurien
927 supérieur d'Europe. PhD thesis, University Lyon 1, Lyon, 2 Volumes, 534 pp.
928 (unpublished). [In French].
929 Perrier, V., 2012. An atypical Silurian myodocope ostracod from the Armorican Massif,
930 France. Acta Palaeontologica Polonica 57 363-73.
931 Perrier, V., Bogolepova, O.K., Gubanov, A.P., Siveter, D.J., Williams, M., 2014b. A pelagic
932 myodocopid ostracod from the Silurian of Arctic Russia. Journal of Micropalaeontology
933 34, 51-57.
934 Perrier, V., Olempska, E., Siveter, D.J., Williams, M., Legiot, N., 2019b. Silurian myodocope
935 Ostracods from Poland. Acta Paleontologica Polonica 64, 379-397.
936 https://doi.org/10.4202/app.00552.2018.

937 Perrier, V., Siveter, D.J., 2013. The use of 'European' ostracode faunas in testing Silurian
938 stratigraphy and palaeogeography. In: Harper, D.A.T., Servais, T. (Eds), Early Palaeozoic
939 Biogeography and Palaeogeography. Geological Society, London, Memoirs 38, 347-56.
940 Perrier, V., Siveter, D.J., Williams, M., Lane, P.D., 2014c. An Early Silurian 'Herefordshire'
941 myodocope ostracod from Greenland and its palaeoecological and palaeobiogeographical
942 significance. Geological magazine 151, 591-599.
943 Perrier, V., Siveter, D.J., Williams, M., Palmer, D. 2019a. British Silurian Myodocopes.
944 Monograph of the Palaeontographical Society 172, 1-105.
945 Perrier, V., Siveter, D.J., Williams, M., Strusz, D.L. Steeman, T., Verniers, J.,
946 Vandenbroucke, T.R.A., 2014a. Myodocope ostracods from the Silurian of Australia.
947 Journal of Systematic Palaeontology 13, 727-739.
948 Perrier, V., Vannier, J., Siveter, D.J., 2007. The Silurian pelagic myodocope ostracod
949 Richteria migrans. Transactions of the Royal Society of Edinburgh, Earth Sciences 98, 1-
950 13.
951 Perrier, V., Vannier, J., Siveter, D.J., 2011. Silurian bolbozoids and cypridinids (Myodocopa)
952 from Europe: pioneer pelagic ostracods. Palaeontology 54 (6), 1361-1391.
953 Perrier, V., Williams, M., Siveter, D.J., 2015. The fossil record and palaeoenvironmental
954 significance of marine arthropod zooplankton. Earth-Science Reviews 146, 146-62.
955 Perrier, V., Williams, M., Siveter, D.J., Palmer, D., Steeman, T., Vandenbroucke, T.R.A.,
956 2019c. A high-precision global biostratigraphy of myodocope ostracods for the Silurian
957 upper Wenlock Series and Ludlow Series. Lethaia 53 (3), 295-309.
958 Pokorný, V., 1958. Grundzüge der zoologischen Mikropaläontologie Bd. 2. Deutscher Verlag
959 der Wissenschaften, Berlin, 582 pp. [In German].
960 Přibyl, A., 1950. On the Bohemian Ostracoda of the families Entomozoidae and
961 Entomoconchidae. Bulletin international de l'Académie tchèque des Sciences 1949, 1-28.

962 Přibyl, A., 1988. Ostracodes from the Silurian of central Bohemia. Sbornik geologicky věd
963 Paleontologie 29, 49-143.
964 Raiswell, R., Fisher, Q.J., 2000. Mudrock-hosted carbonate concretions: a review of growth
965 mechanisms and their influence on chemical and isotopic composition: Journal of the
966 Geological Society, 157, 239–251.
967 Robardet, M., Gutiérrez-Marco, J.C., 2002. Silurian. Chapter 5 In: Gibbons, W., Moreno, T.
968 (Eds.), The Geology of Spain. The Geological Society, London, 51-66.
969 Robardet, M., Gutiérrez-Marco, J.C., 2004. The Ordovician, Silurian and Devonian sedimentary
970 rocks of the Ossa-Morena Zone (SW Iberian Peninsula, Spain). Journal of Iberian Geology
971 30, 73-92.
972 Robardet, M., Rábano, I., Gutiérrez-Marco, J.C., Sarmiento, G.N., Vaněk, J., 2000. La "Caliza
973 de *Scyphocrinites*" (Silúrico superior) del norte de Sevilla: avance de resultados
974 paleontológicos y bioestratigráficos. In: Díez, J.B., Balbino, A.C. (Eds), Resumos I
975 Congresso Ibérico de Paleontología y XV Jornadas de la Sociedad Española de
976 Paleontología (ISBN 972-778-026-1), Évora, 270-272. [In Spanish].
977 San José, M.A. de, Herranz, P., Pieren, A.P., 2004. A review of the Ossa-Morena Zone and its
978 limits. Implications for the definition of the Lusitan-Marianic Zone. Journal of Iberian
979 Geology 30, 7-22.
980 Sarmiento, G.N., Piçarra, J.M., Rebelo, J.A., Robardet, M., Gutiérrez-Marco, J.C., Štorch, P.,
981 Rábano, I., 1999. Le Silurien du synclinorium de Moncorvo (NE du Portugal) :
982 biostratigraphie et importance paléogéographique. Geobios 32 (5), 749-767. [In French].
983 Sars, G.O., 1866. Oversigt af Norges marine Ostracoder. Norske Videnskcaps-Akademien
984 Forhandlingar, 1865, 130 pp. [In Danish].

985 Schmidt, H., 1931. Das Paläozoikum des Spanischen Pyrenäen. Abhandlungen der
986 Gessellschaft der Wissenschaften zu Göttingen, Mathematik-Physik Klasse 3 [H 5], 8,
987 981-1065. [In German].
988 Scotese, C.R., 2016. PALEOMAP PaleoAtlas for GPlates and the PaleoData Plotter Program,
989 PALEOMAP Project, http://www.earthbyte.org/paleomap-paleoatlas-for-gplates/
990 Seilacher, A., Hauff, R.B., 2004. Constructional morphology of pelagic crinoids. Palaios, 19,
991 3-16.
992 Simon, W., 1951. Untersuchungen im Paläozoikum von Sevilla (Sierra Morena, Spanien).
993 Abhandlungen der Senckenbergischen Naturforschenden Gesellschaft, 485, 31-52. [In
994 German].
995 Siveter, D.J., 1982. Casts illustrating fine ornament of a Silurian ostracod. In Bate, R.H.,
996 Robinson, E., Sheppard, L.M. (Eds): Fossil and Recent Ostracods. British
997 Micropalaeontological Society, Ellis Horwood, Chichester, 105-22.
998 Siveter, D.J., 1984. Habitats and modes of life of Silurian ostracods. In: Bassett, M.G.,
999 Lawson J.D. (Eds), The Autecology of Silurian Organisms. Special Papers in
1000 Palaeontology, 32, 71-85.
1001 Siveter, D.J., Perrier, V., Williams, M., 2022. Silurian myodocopes display adaptations for a
1002 nektobenthic lifestyle: The paleobiological evidence. Marine Micropaleontology 174,
1003 101906.
1004 Siveter, D.J., Vannier, J., 1990. The Silurian myodocopid ostracode *Entomozoe* from the
1005 Pentland Hills, Scotland; its taxonomic, ecological and phylogenetic significance and the
1006 systematic affinity of the bolbozoid myodocopids. Transactions of the Royal Society of
1007 Edinburgh, Earth Sciences 81, 45-67.

1008 Siveter, D.J., Vannier, J., Palmer, D., 1987. Silurian myodocopid ostracodes: their
1009 depositional environment and the origin of their shell microstructures. Palaeontology 30,
1010 783-813.
1011 Siveter, D.J., Vannier, J., Palmer, D., 1991. Silurian myodocopes: Pioneer pelagic ostracodes
1012 and the chronology of an ecological shift. Journal of Micropalaeontology 10, 151-173.
1013 Torsvik, T., Cocks, L.R.M., 2013. New global palaeogeographical reconstructions for the
1014 Early Palaeozoic and their generation. In Harper, D.A.T. & Servais, T. (eds): Early
1015 Palaeozoic Biogeography and Palaeogeography. Geological Society of London, Memoirs
1016 38, 5-24.
1017 Vannier, J., 1987. On *Calocaria maurae*. Stereo-Atlas of Ostracod Shells 14, 45-8.
1018 Vannier, J., Abe, K., 1992. Recent and early Palaeozoic myodocope ostracodes: functional
1019 morphology, phylogeny, distribution and lifestyles. Palaeontology 3, 485-517.
1020 Vannier, J., Abe, K., Ikuta, K., 1998. Feeding in myodocopid ostracods: functional
1021 morphology and laboratory observations from videos. Marine Biology 132, 391-408.
1022 Wang, Shang-qi., 1989. Early Devonian ostracodes from Zhangmu of Yulin, Guangxi. Acta
1023 Palaeontologica Sinica 28, 249–268. [in Chinese].
1024 Wang, Shang-qi., 2009. Palaeozoic Entomozoacea and Leperditicopida (Ostracoda) of China.
1025 Fossil Ostracoda of China, 3, 251 pp. [In Chinese].
1026 Wang, Shang-qi, Zhang, Xiao-bin., 1983. Ostracodes from Lower and Middle Devonian of
1027 the Luofu and other areas, Guangxi Province. Acta Palaeontologica Sinica 22, 551-565. [In
1028 Chinese].
1029 Weitschat, W., 1983. On *Triadocypris spitzbergensis* Weitschat. A stereo-atlas of ostracod
1030 shells 10, 127-138.
1031 Wilby, P.R., Wilkinson, I.P., Riley, N.J., 2005. Late Carboniferous scavenging ostracods:
1032 feeding strategies and taphonomy. Earth and Environmental Science Transactions of the

Royal Society of Edinburgh 96(4), 309-316.

Wilkinson, I.P., Williams, M., Siveter, D.J., Wilby, P.R., 2004. A Carboniferous necrophagous myodocopid ostracod from Derbyshire, England. Revista Española de Micropaleontología 36, 195-206.

Yoshida, H., Yamamoto, K., Minami, M., Katsuta, N., Sin-Ichi, S., Metcalfe, R. 2018. Generalized conditions of spherical carbonate concretion formation around decaying organic matter in early diagenesis. Scientific reports 8(1), 6308.

Zanina, I.E., Polenova, E.N., 1960. Subclass Ostracoda. Členistonogie. Trilobitoobraznye i rakoobraznye, 515.

Figures explanation

Fig. 1. Geographic location and lithology of Mina Guillermín locality, Alcaracejos, province of Córdoba, Andalusia, southern Spain. **A.** Location of the studied area in the Iberian Peninsula within Spain. **B.** Geological map of the area showing the three mains geological domains of the Córdoba region. **C.** Extract of the 1:50 000 geological map of Espiel with the precise location of the outcrop. **D.** General stratigraphic log and lithology of the Calatraveño anticline. **E-G.** Lithology of the Mina Guillermín outcrop. **E.** General view of the outcrop. **F.** Detail of the *Scyphocrinites* bearing nodules. **G.** Detail of the black/reddish shales. A-D, Star indicating the position of the locality; B-D, after Mapa Geológico de España 1: 50 000, sheet 880, Espiel (Apalategui Isasa et al. 1985).

Fig. 2. Lateral views of selected myodocope specimens from the shales of Mina Guillermín locality, Alcaracejos, Córdoba province, southern Spain; Pridoli Series, Silurian. **A.** MGM-8043S, *Bolbozoe anomala*, left valve. **B.** MGM-8044S, *B. anomala*, right valve

showing post-mortem diagenetic features. **C.** MGM-8045S, *B. anomala*, right valve. **D.** MGM-8046S, *Silurocypridina calva*, right valve. **E.** MGM-8047S, *S. calva*, left valve. **F.** MGM-8048S, *S. calva*, right valve. **G.** MGM-8049S, *Nudator angiportatus*, left valve. **H.** MGM-8050S, *S. variostriata*, right valve. **I.** MGM-8051S, *S. variostriata*, right valve. **J.** MGM-8052S, *Sineruga insolita*, right valve. All are light pictures; A, B, E-I are latex casts of external moulds.

Fig. 3. Selected *Bolbozoe* specimens from the nodules of Mina Guillermín locality, Alcaracejos, Córdoba province, southern Spain; Pridoli Series, Silurian. **A.** MGM-8053S, *Bolbozoe anomala*, left valve, lateral view. **B-D.** MGM-8054S, *B. anomala*, left valve. **B.** lateral view; **C.** lateroventral view; **D.** detail of the adductorial muscle scar. **E.** MGM-8055S, *B. anomala*, left valve, lateral view. **F-I.** MGM-8056S, *B.* aff. *rugosa*, left valve. **F.** lateral view; **G.** dorsolateral view; **H.** lateral view of a cast of the counterpart; I. detail of the adductorial muscle scar. All are light pictures; F, G are stereopairs; H, I are latex casts of external moulds.

Fig. 4. Selected *Boucia ornatissima* specimens from the nodules of Mina Guillermín locality (A-C), Alcaracejos, Córdoba province, southern Spain and from the Prague Basin (D-L), Czech Republic; Pridoli Series, Silurian. **A.** MGM-8057S, left valve, lateral view. **B.** MGM-8058S, right valve, lateral view. **C.** MGM-8059S, incomplete left valve, lateral view. **D.** NM-L 28477, open carapace in butterfly position, lateral view. **E.** NM-L 14041, Paratype, left valve, lateral view. **F.** NM-L 14021, Holotype, right valve, lateral view. **G, H, K**. FSL 71798, left valve. **G.** lateral view; **H.** detail of the ventral margin; **K.** detail of the posterodorsal margin. **I, J, L**. FSL 71797, right valve. **I.** lateral view; **J.** detail of the dorsal

margin; **K.** frontal view. All are light pictures; A, B, G-L are stereopairs; C is a latex cast of an external mould.

Fig. 5. Idealised reconstructions of *Boucia ornatissima*.

Fig. 6. Selected *Silurocypridina calva* specimens from the nodules of Mina Guillermín locality, Alcaracejos, Córdoba province, southern Spain; Pridoli Series, Silurian. **A.** MGM-8060S, right valve, frontal view. **B.** MGM-8061S, right valve, lateroventral view. **C-E**. MGM-8062S, right valve. **C.** lateral view; **D.** frontal view; **E.** lateroventral view. **F.** MGM-8063S, right valve, lateral view. All are stereopairs of light pictures; A-E are latex casts of external moulds.

Fig. 7. Selected *Calocaria maurae* specimens from the nodules of Mina Guillermín locality, Alcaracejos, Córdoba province, southern Spain; Pridoli Series, Silurian. **A, B.** MGM-8064S, right valve. **A.** lateral view; **B.** ventral view. **C-D**. MGM-8065S, right valve. **C.** lateral view; **D.** frontal view. **E, F.** MGM-8066S, left valve. **E.** lateral view; **F.** frontal view. **G.** MGM-8067S, left valve, posterior view. All are stereopairs of light pictures; C, D are latex casts of external moulds.

Fig. 8. Selected *Calocaria robusta* specimens from the nodules of Mina Guillermín locality, Alcaracejos, Córdoba province, southern Spain; Pridoli Series, Silurian. **A, D.** MGM-8068S, right valve. **A.** lateral view; **D.** detail of the anterior part of the valve in lateral view. **B**. MGM-8069S, incomplete right valve, posterior view. **C, E.** MGM-8070S, incomplete left valve. **C.** lateral view; **E.** detail of the ventral part of the valve in lateral view. All are light pictures of latex casts of external moulds; A-C are stereopairs.

Fig. 9. Selected *Calocaria callundosa* sp. nov. specimens from the nodules of Mina Guillermín locality, Alcaracejos, Córdoba province, southern Spain; Pridoli Series, Silurian. **A, B.** MGM-8071S, Holotype, right valve. **A.** lateral view; **B.** lateroventral view. **C-G.** MGM-8072S, left valve. **C.** frontal view; **D.** lateral view; **E.** dorsal view; **F.** lateroventral view; **G.** posterolateral view. All are stereopairs of light pictures; A, B are latex casts of external moulds.

Fig. 10. Shales and nodules myodocope assemblages of Mina Guillermín locality, Alcaracejos, Córdoba province, southern Spain; Pridoli Series, Silurian.

Fig. 11. Measurements (length/height) of *B. anomala* and *S. calva* specimens from the shales and nodules assemblages of Mina Guillermín locality, Alcaracejos, Córdoba province, southern Spain; Pridoli Series, Silurian.

Fig. 12. Artistic reconstruction of the possible late Silurian pelagic ecosystem at Mina Guillermín locality. The *Scyphocrinites* are represented within the upper part of the water column following the hypothesis of Seilacher and Hauff (2004). Drawing and conceptualization by VP.

Fig. 13. Stratigraphical and palaeogeographical distribution of Pridoli myodocope faunas from Spain, France, Sardinia and Czech Republic. **A.** Stratigraphical distribution of Pridoli myodocope species. **B.** Palaeogeographical position of Pridoli myodocope-bearing outcrops and close up on the North Gondwanan margin (420Ma). B, map after Scotese (2016) and

approximate latitude from Torsvik and Cocks (2013). Lud. = Ludlow; Ludf. = Ludfordian; Jarov. = Jarovian; Rado. = Radotinian.

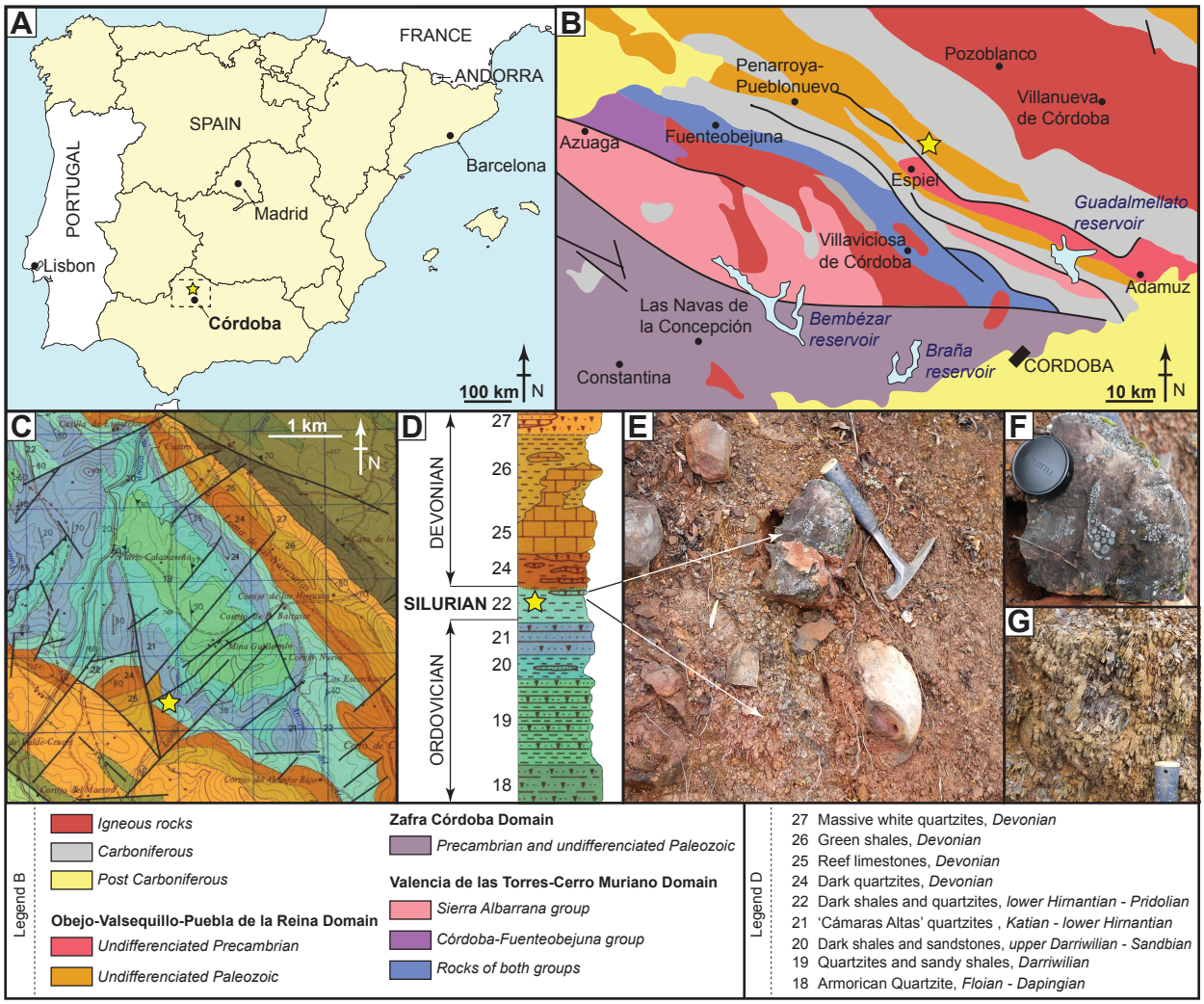
A
FRANCE
ANDORRA
SPAIN
PORTUGAL
Barcelona
Madrid
Lisbon
Córdoba
100 km
N
B
Pozoblanco
Penarroya-
Pueblonuevo
Villanueva
de Córdoba
Azuaga
Fuenteobejuna
Espiel
Guadalmellato
reservoir
Villaviciosa
de Córdoba
Adamuz
Las Navas de
la Concepción
Bembézar
reservoir
Braña
reservoir
Constantina
CORDOBA
10 km
N
C
1 km
N
D
DEVONIAN
SILURIAN
ORDOVICIAN
27
26
25
24
22
21
20
19
18
E
F
G
Legend B
Igneous rocks
Carboniferous
Post Carboniferous
Obejo-Valsequillo-Puebla de la Reina Domain
Undifferenciated Precambrian
Undifferenciated Paleozoic
Zafra Córdoba Domain
Precambrian and undifferenciated Paleozoic
Valencia de las Torres-Cerro Muriano Domain
Sierra Albarrana group
Córdoba-Fuenteobejuna group
Rocks of both groups
Legend D
27 Massive white quartzites, Devonian
26 Green shales, Devonian
25 Reef limestones, Devonian
24 Dark quartzites, Devonian
22 Dark shales and quartzites, lower Hirnantian - Pridolian
21 'Cámaras Altas' quartzites , Katian - lower Hirnantian
20 Dark shales and sandstones, upper Darriwilian - Sandbian
19 Quartzites and sandy shales, Darriwilian
18 Armorican Quartzite, Floian - Dapingian

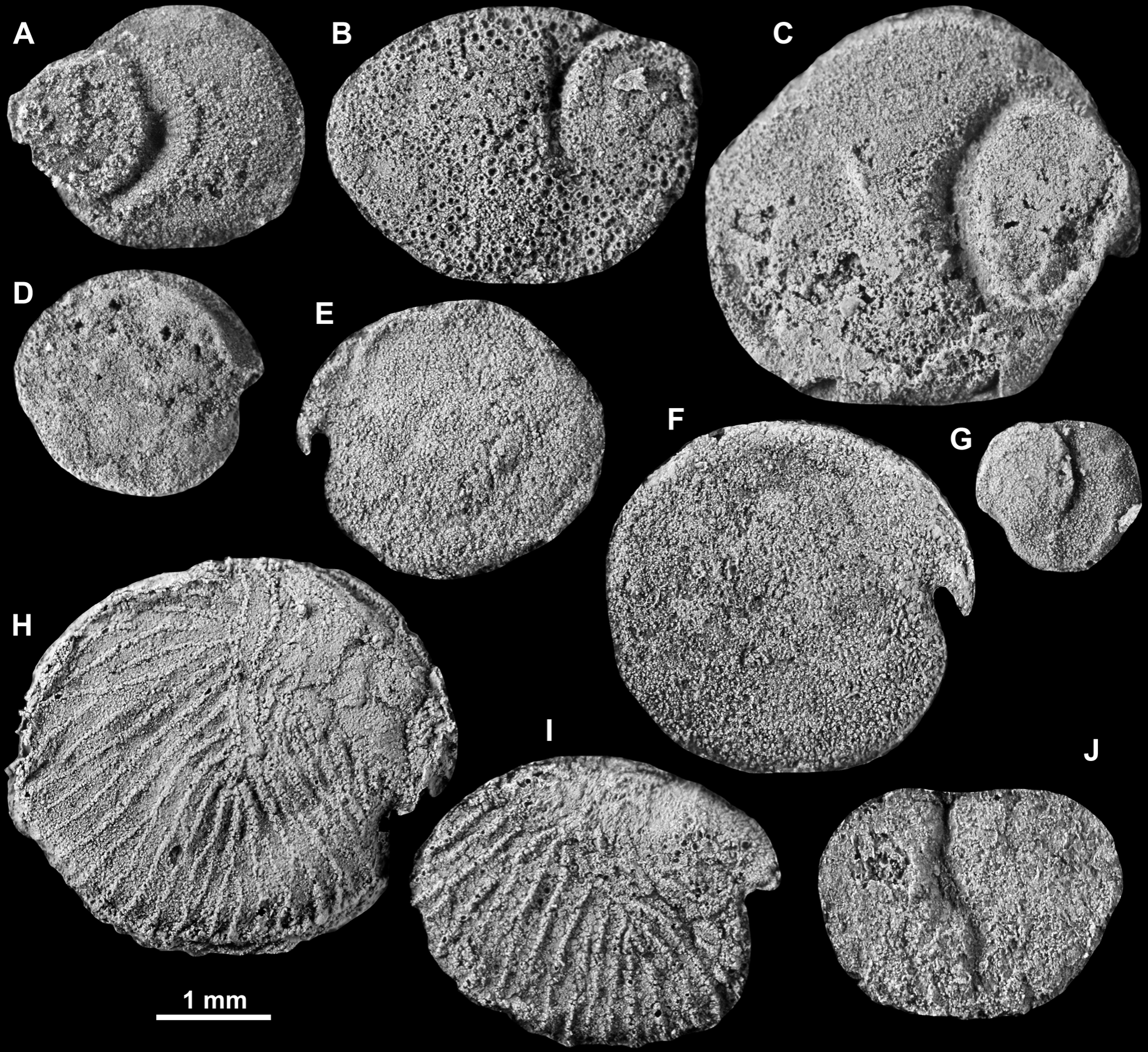
A
B
C
D
E
F
G
H
I
J
1 mm

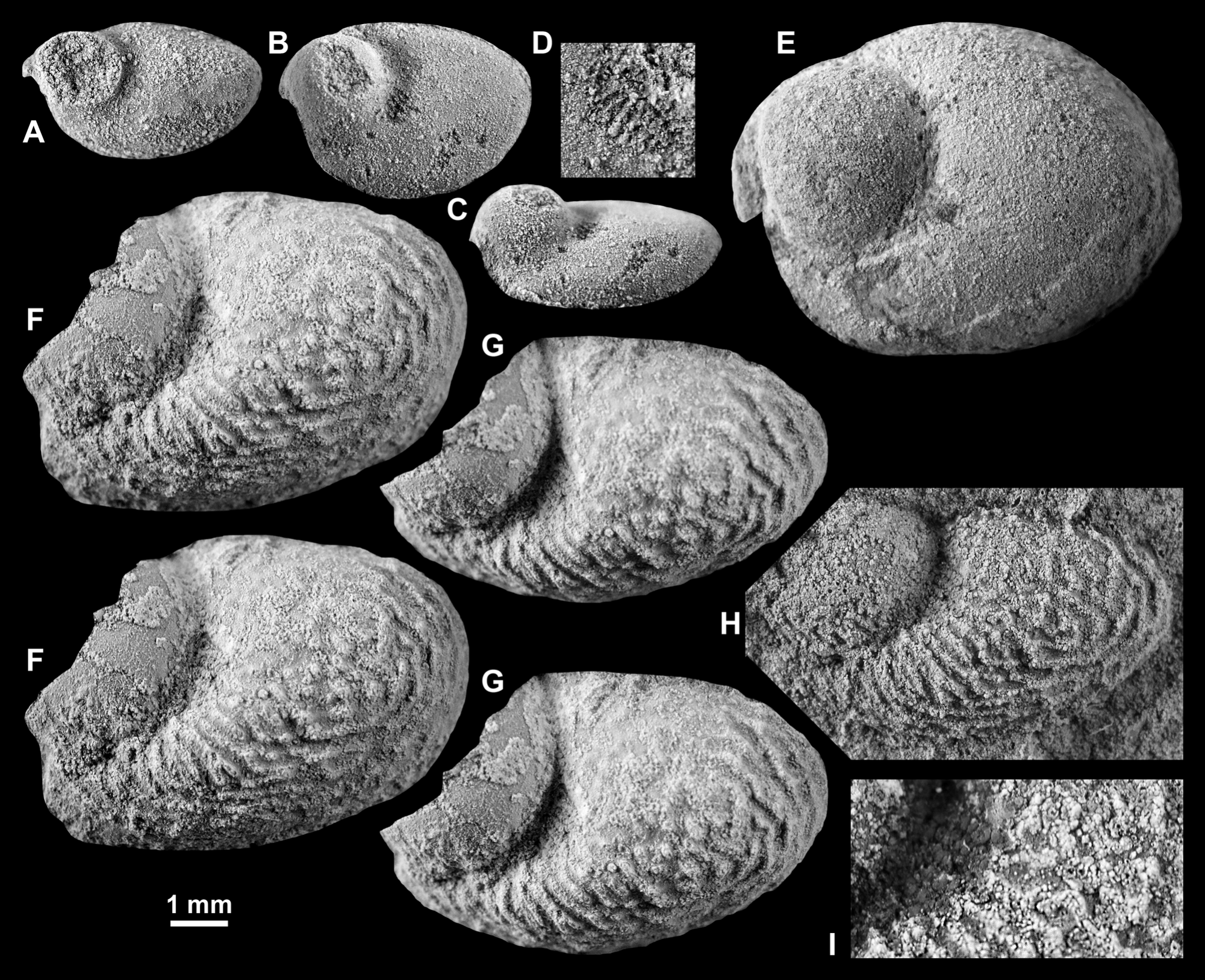
A
B
D
E
C
F
G
F
G
H
I
1 mm


A
B
A
B
C
D
E
F
1mm
G
H
I
J
K
L
G
H
I
J
K
L

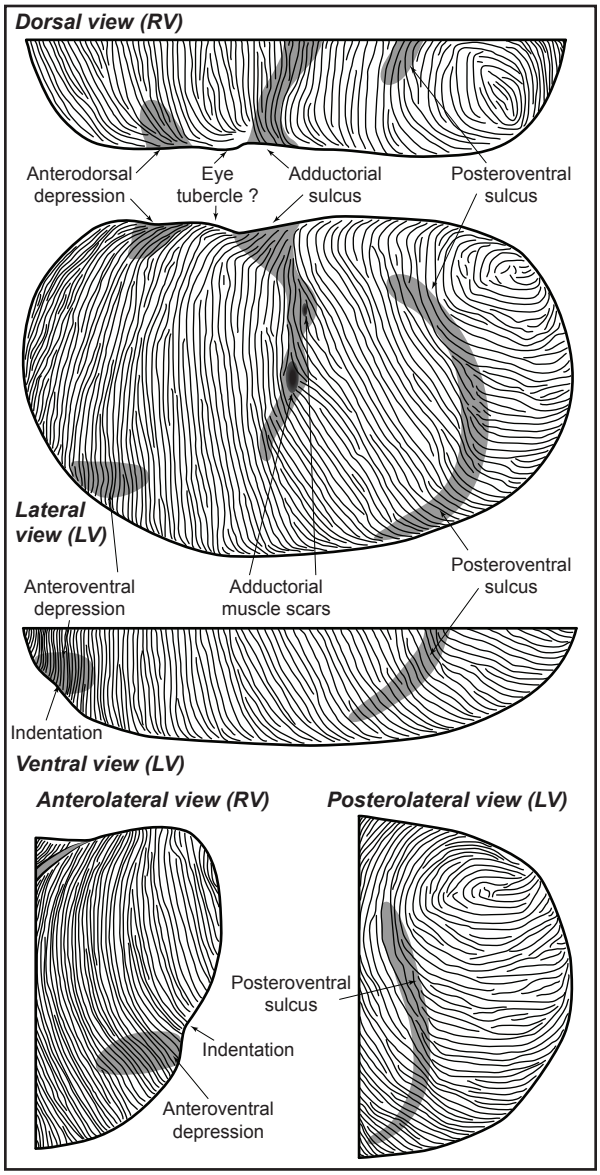
Dorsal view (RV)
Anterodorsal depression
Eye tubercle ?
Adductorial sulcus
Posteroventral sulcus
Lateral view (LV)
Anteroventral depression
Adductorial muscle scars
Posteroventral sulcus
Indentation
Ventral view (LV)
Anterolateral view (RV)
Posterolateral view (LV)
Posteroventral sulcus
Indentation
Anteroventral depression

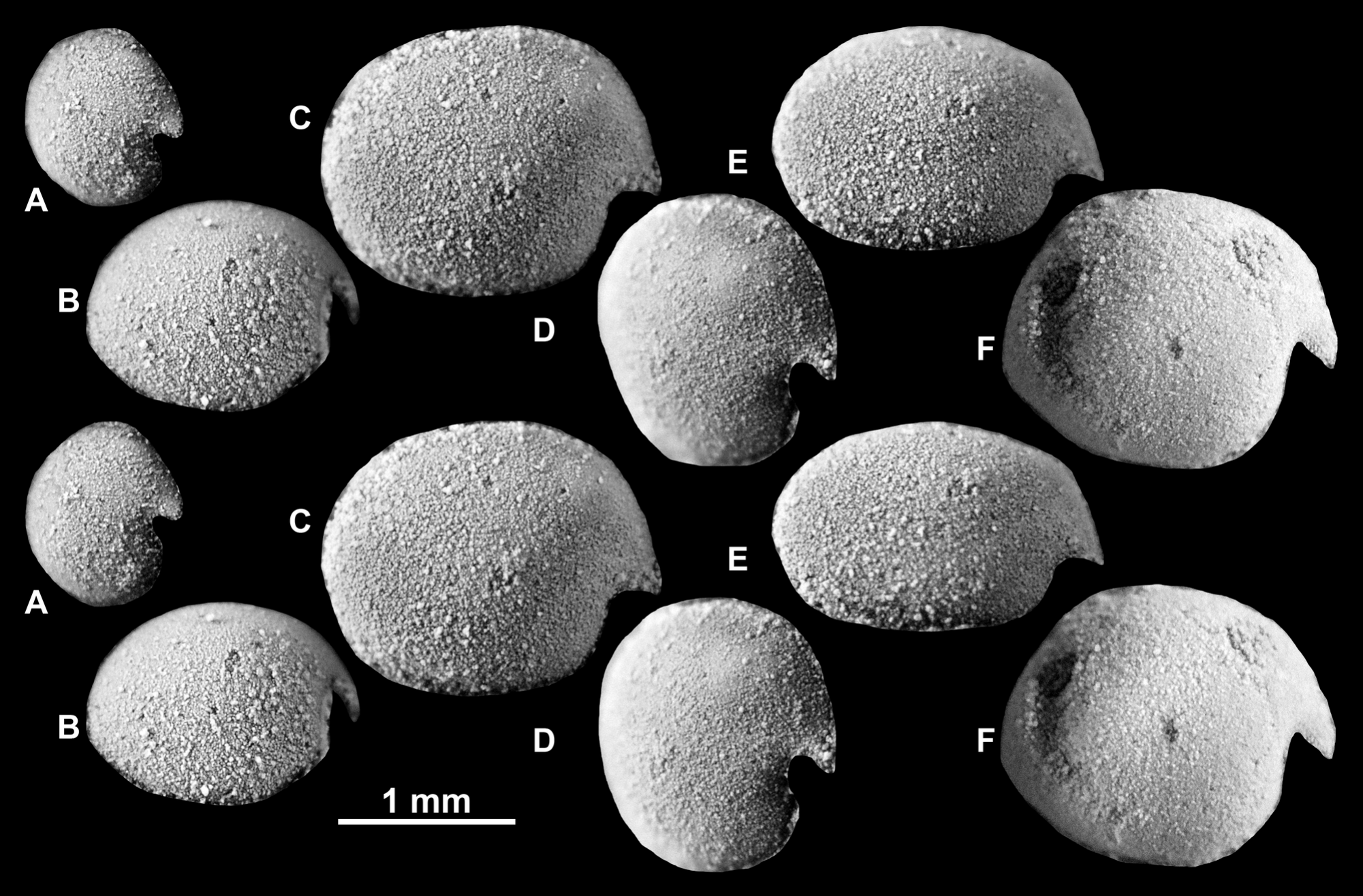
A
B
C
D
E
F
A
B
C
D
E
F
1 mm

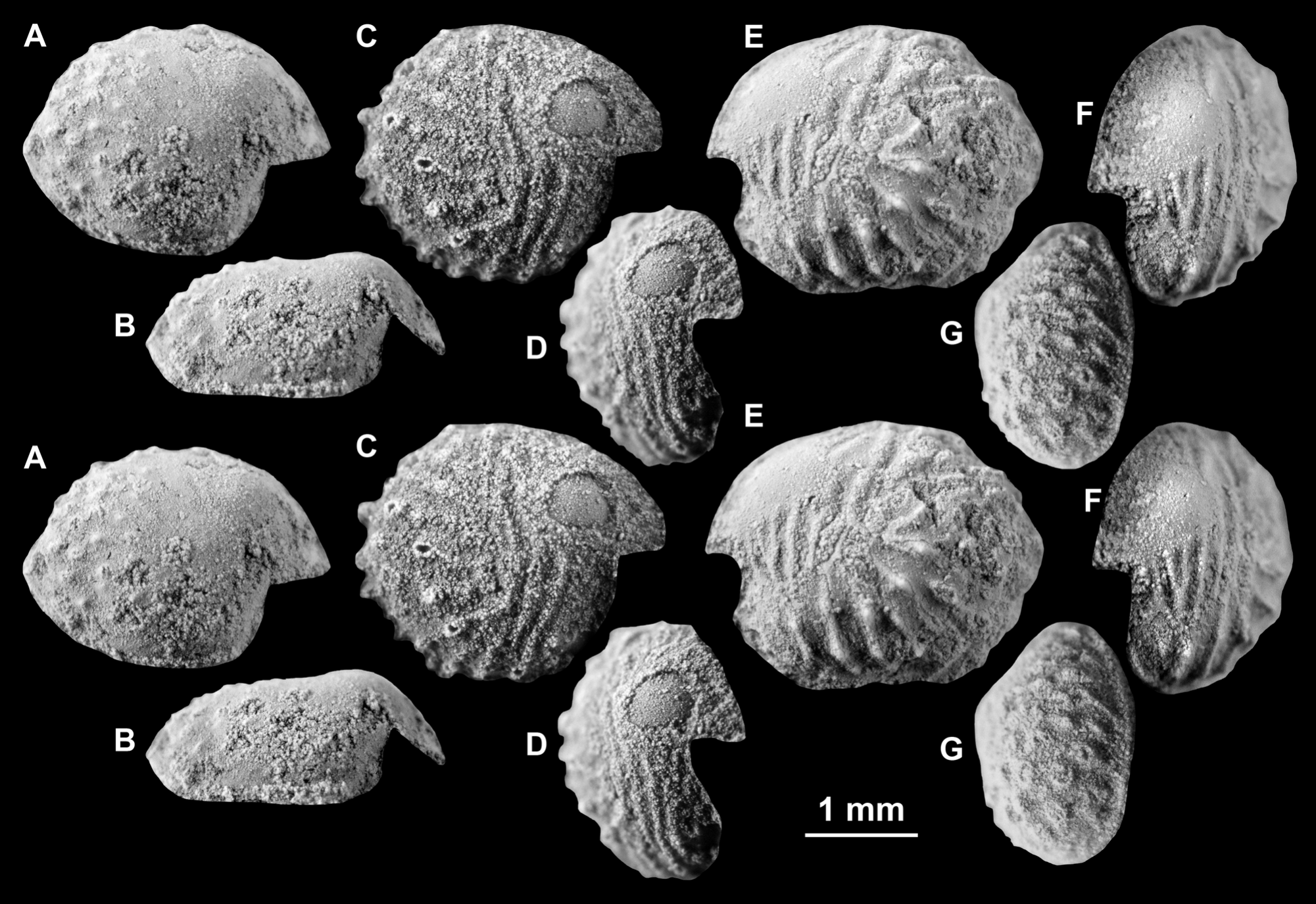
A
B
C
D
E
F
G
A
B
C
D
E
F
G
1 mm

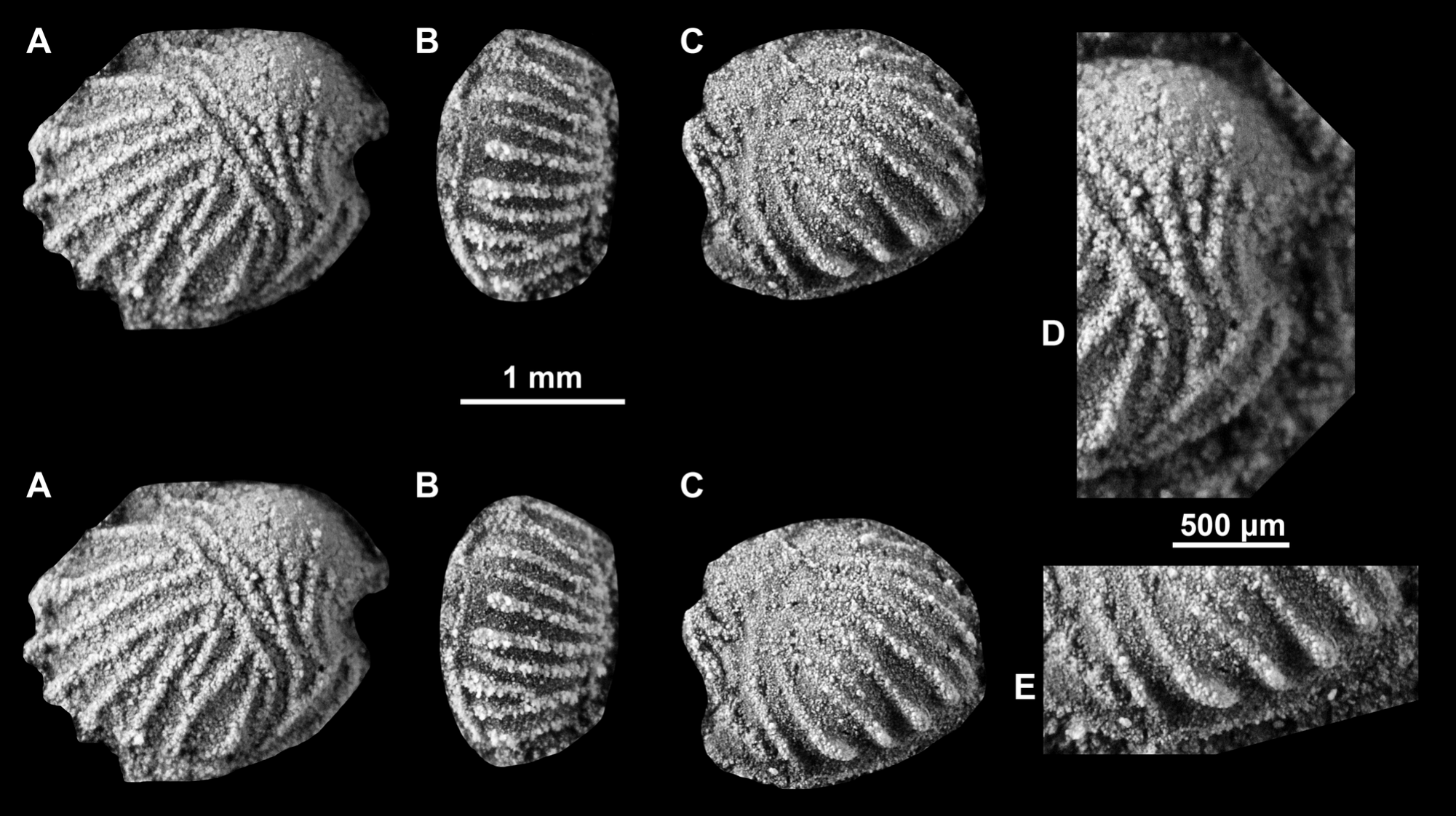
A
B
C
D
1 mm
A
B
C
500 µm
E

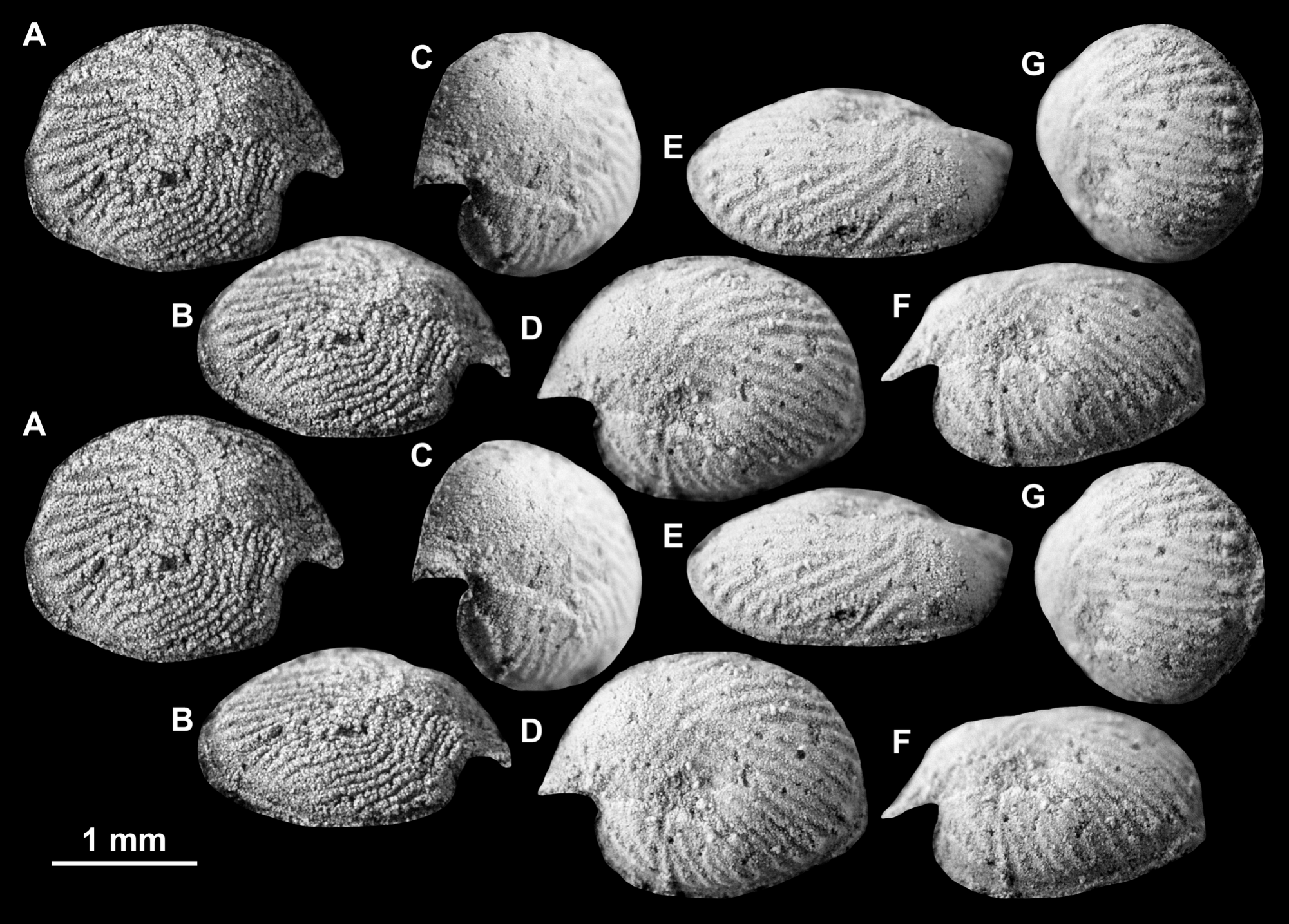
A
C
G
E
B
D
F
A
C
G
E
B
D
F
1 mm

Species	Shales specimens	Shales %	Nodules specimens	Nodules %	Total specimens
Bolbozoe anomala	280	63,9	58	11,2	**338**
Bolbozoe aff. *rugosa*	0	0	5	1	**5**
Nudator angiportatus	6	1,4	0	0	**6**
Sineruga insolita	3	0,7	0	0	**3**
Boucia ornatissima	0	0	4	0,8	**4**
Silurocypridina calva	124	28,3	250	48,4	**374**
Silurocypridina variostriata	25	5,7	0	0	**25**
Calocaria maurae	0	0	85	16,5	**85**
Calocaria robusta	0	0	92	17,8	**92**
Calocaria callundosa sp. nov.	0	0	22	4,3	**22**
Totals	**438**	100	**516**	100	**954**

Ostracod species and faunal composition (based on 438 specimens) from the **shales** of la Mina Guillermin Alcaracejos, Córdoba district, central Spain.

A, *B. anomala*
B, *S. calva*
C, *S. variostriata*
D, *N. angiportatus*
E, *S. insolita*

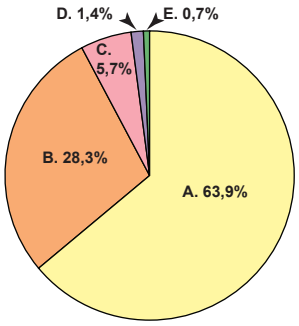

Ostracod species and faunal composition (based on 516 specimens) from the **nodules** of la Mina Guillermin Alcaracejos, Córdoba district, central Spain.

A, *S. calva*
B, *C. robusta*
C, *C. maurae*
D, *B. anomala*
E, *C. callundosa* sp. nov.
F, *B.* aff. *rugosa*
G, *B. ornatissima*

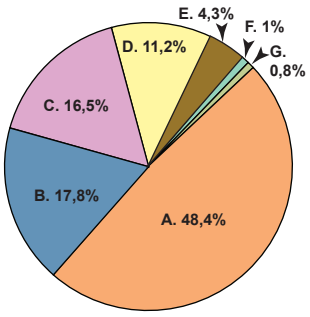

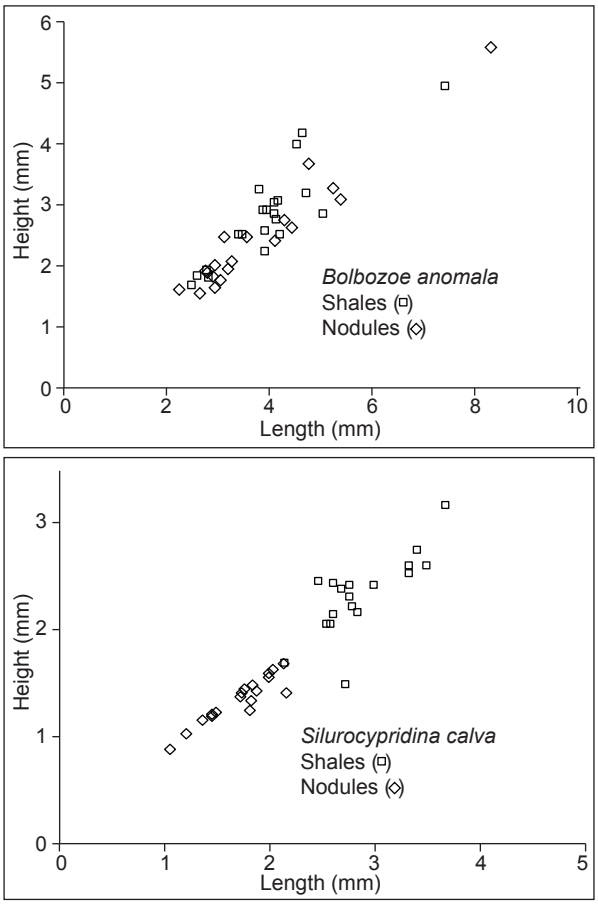
Height (mm)
Length (mm)
0
1
2
3
4
5
6
0
2
4
6
8
10
Bolbozoe anomala
Shales (□)
Nodules (◇)

Height (mm)
Length (mm)
0
1
2
3
0
1
2
3
4
5
Silurocypridina calva
Shales (□)
Nodules (◇)

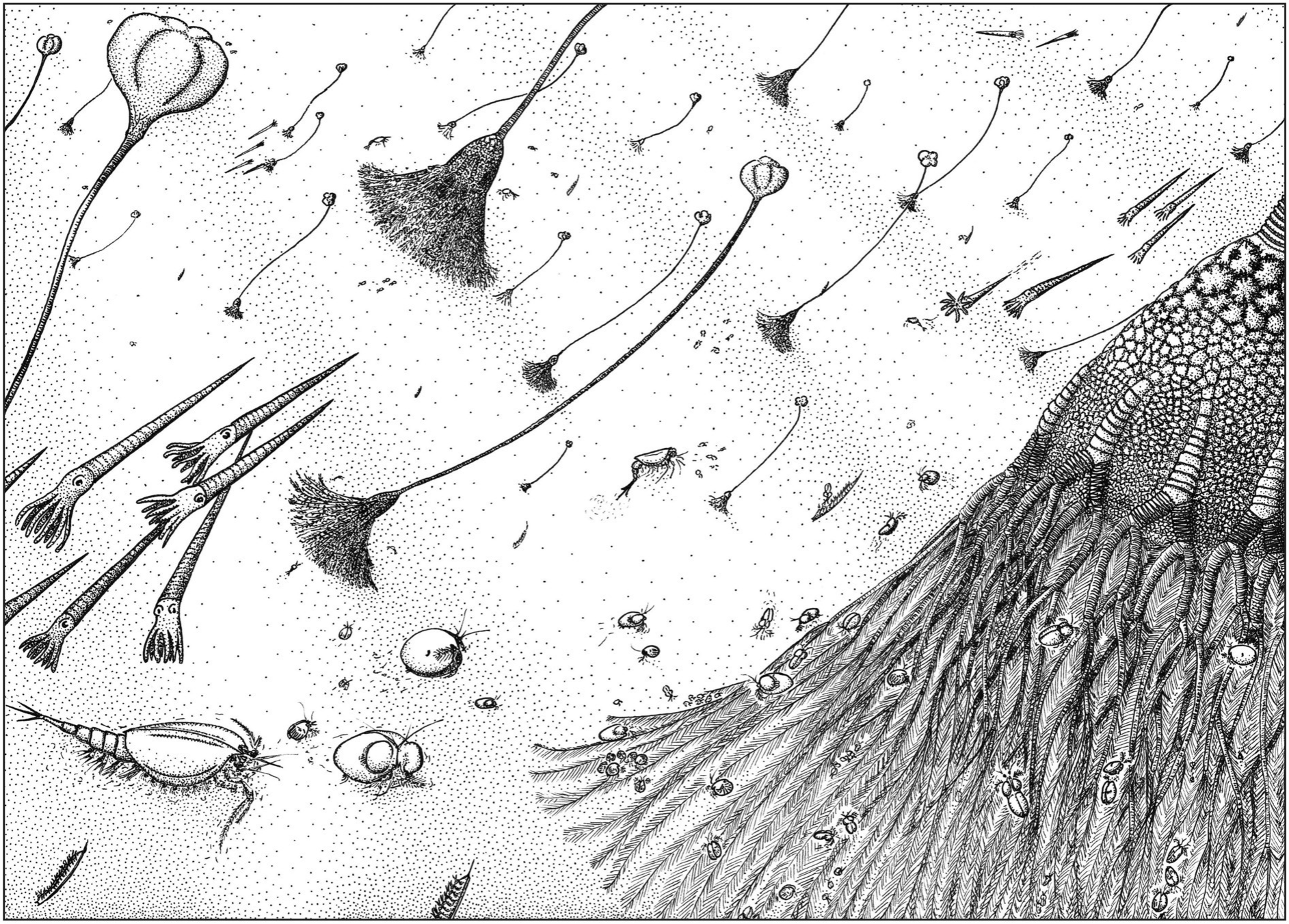

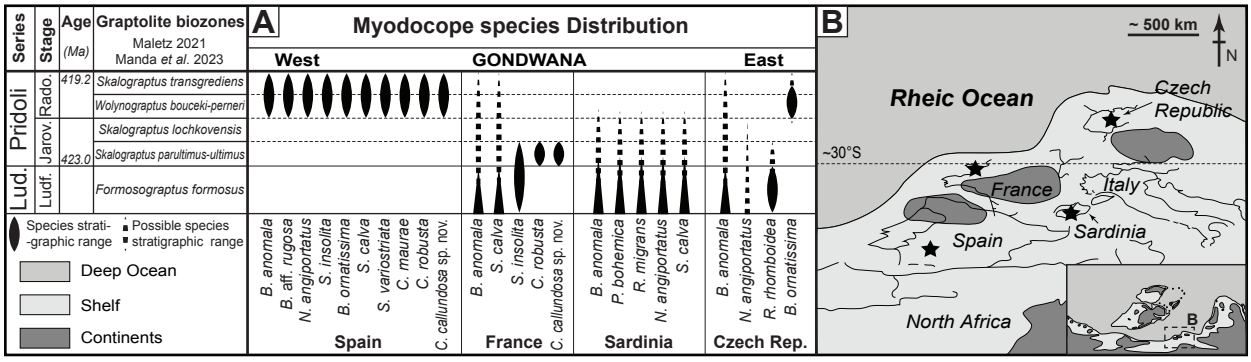
Series
Stage
Age (Ma)
Graptolite biozones
Maletz 2021
Manda et al. 2023
Pridoli
Lud.
Rado.
Jarov.
Ludf.
419.2
423.0
Skalograptus transgrediens
Wolynograptus boucekí-perneri
Skalograptus lochkovensis
Skalograptus parultimus-ultimus
Formosograptus formosus
Species stratigraphic range
Possible species stratigraphic range
Deep Ocean
Shelf
Continents
A
Myodocope species Distribution
West
GONDWANA
East
B. anomala
B. aff. rugosa
N. angiportatus
S. insolita
B. ornatissima
S. calva
S. variostriata
C. maurae
C. robusta
C. callundosa sp. nov.
Spain
France
Sardinia
Czech Rep.
P. bohemica
R. migrans
R. rhomboidea
B
~ 500 km
N
Rheic Ocean
Czech Republic
~30°S
France
Italy
Spain
Sardinia
North Africa